Drag reduction systems towards aeronautical applications

Jacopo Banchetti

Supervisor Maurizio Quadrio

PhD defense, 16/10/2020

Outline

- Introduction
- Preliminary RANS investigation
- Incompressible DNS over a bump
- Transonic DNS over a wing slab
- Blowing actuator

Turbulent skin-friction drag reduction

- Passive Strategies

Riblets

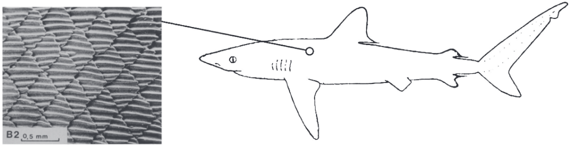

Bechert & Hage, FPN 2006

- Active Strategies

Peristalsis

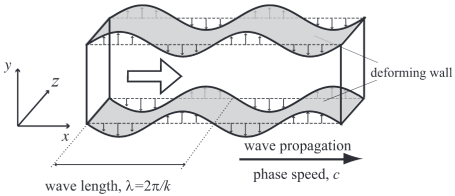

Nakanishi, Mamori & Fukagata, JFM 2012

Turbulent skin-friction drag reduction

Research

- Simple geometries
- Friction drag only
- Low Reynolds number

Applications

- Complex geometries
- Pressure drag - wave drag...
- High Reynolds number

Motivation

What is the effect of friction reduction on the total drag?

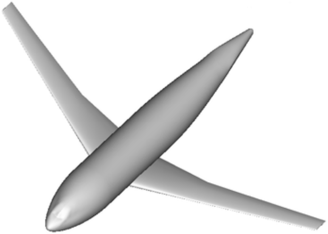

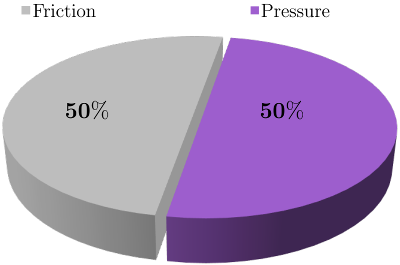

What is the effect of friction reduction on the total drag?

+

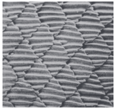

4% of friction reduction

?

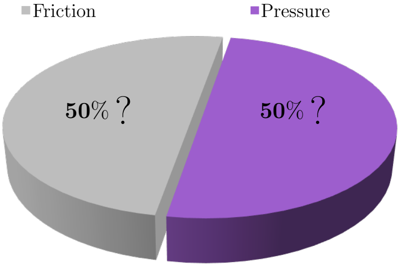

Motivation

What is the effect of friction reduction on the total drag? Extrapolated scenario

+

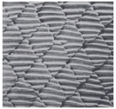

4% of friction reduction

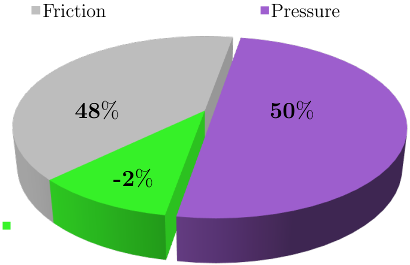

Outline

- Introduction
- Preliminary RANS investigation
- Incompressible DNS over a bump
- Transonic DNS over a wing slab
- Blowing actuator

DLR-F6 is a modern transport aircraft, with a transonic design

- RANS
- Spalart-Allmaras turbulence model
- $Re = 3 \cdot 10^6$, $M = 0.75$
- Reference $C_\ell = 0.5$
- Without (Ref) and with (Control) friction reduction

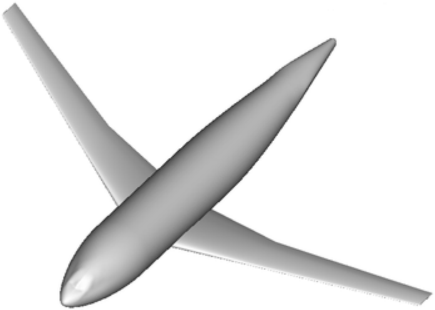

Streamwise-travelling waves of spanwise wall velocity (StTW)

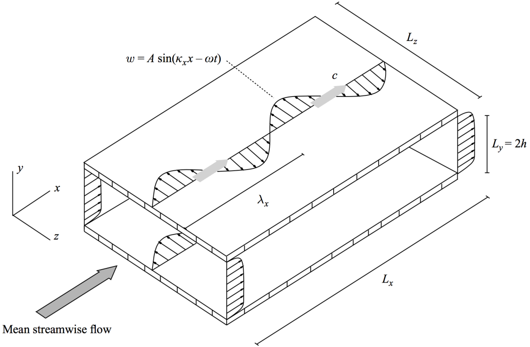

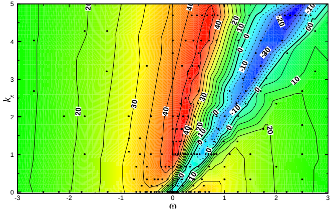

Quadrio, Ricco & Viotti, JFM 2009

Background (Gatti & Quadrio, *JFM*16)

Waves can be assimilated to drag-reducing roughness

- StTW produce a vertical shift ΔB of the logarithmic portion of the mean velocity profile
- ΔB^+ at non-low *Re* becomes Reynolds independent

$$U^+ = \frac{1}{\kappa}\log(y^+) + B + \Delta B^+$$

- Friction reduction over a flat plate at flight-*Re* $> 20\%$

Aircraft forcing

- Forcing is applied over the entire aircraft by a modified wall function

$$U^+ = \frac{1}{\kappa} log(y^+) + B + \Delta B^+$$

- The StTW is supposed to affect the mean velocity profile as over flat walls

- Extrapolated friction reduction of 23%

- Extrapolated total drag reduction around 10%

Friction reduction

- Local friction reduction $\Delta\tau = \frac{\tau^{Ref} - \tau^{StTW}}{\tau^{Ref}}$ around 23%
- Strong variations on the upper wing surface

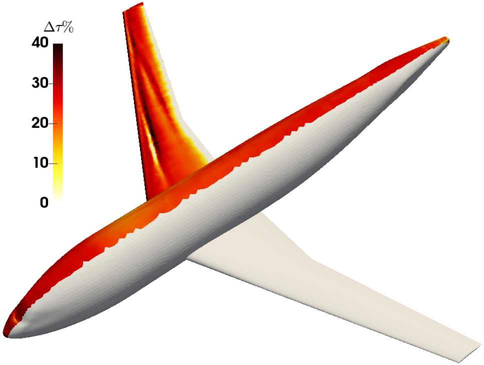

Friction reduction and pressure changes

- Changes on pressure field $\Delta p = \frac{p^{Ref} - p^{StTW}}{p^{Ref}}$ on the upper wing surface
- Negligible variations over the fuselage

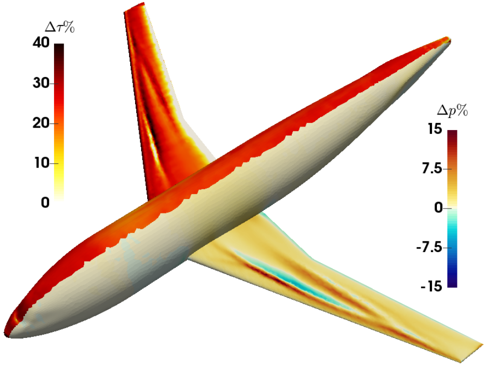

Pressure coefficient

- Shock-wave over the suction side
-

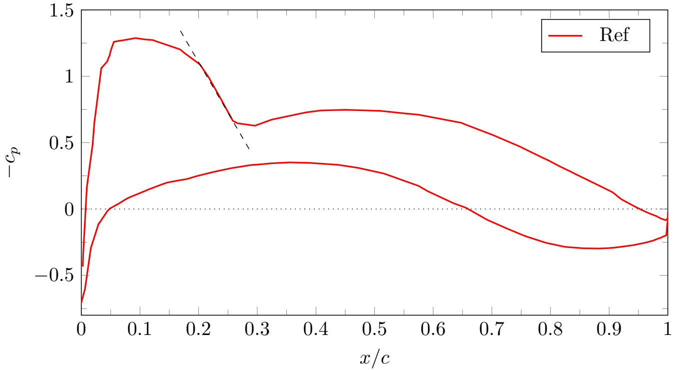

Pressure coefficient

- Shock-wave delay
- Negligible changes over the pressure side

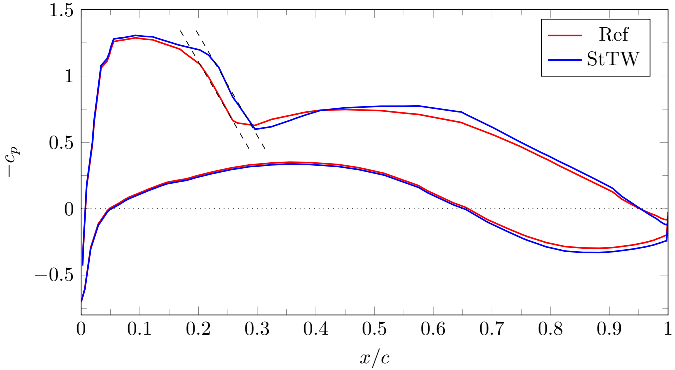

Lift coefficient

- Shock-wave delay
- Lift increase

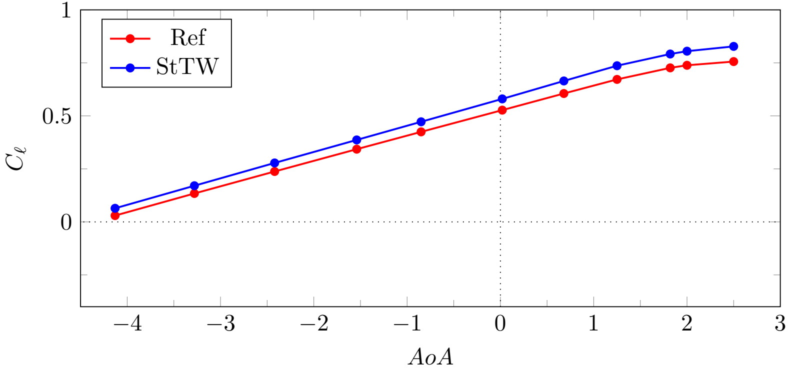

Total drag reduction at constant lift coefficient

- Extrapolated friction reduction of 23%
- Extrapolated total drag reduction around 10%

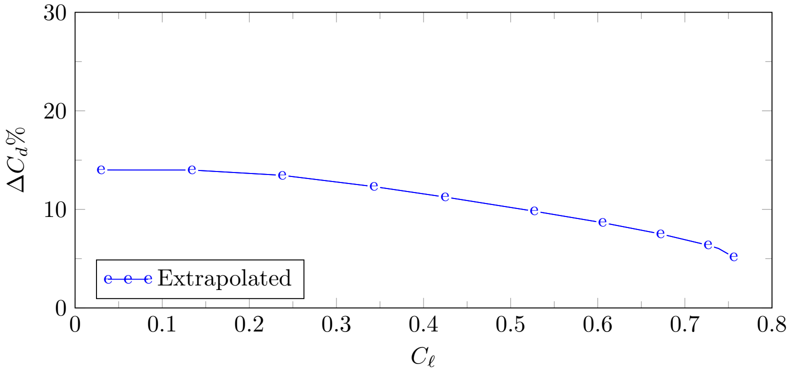

Total drag reduction at constant lift coefficient

- Actual drag reduction is always higher than the extrapolated scenario
- At $C_\ell = 0.5$, $\Delta C_d = 15\%$ instead of the extrapolated 10%

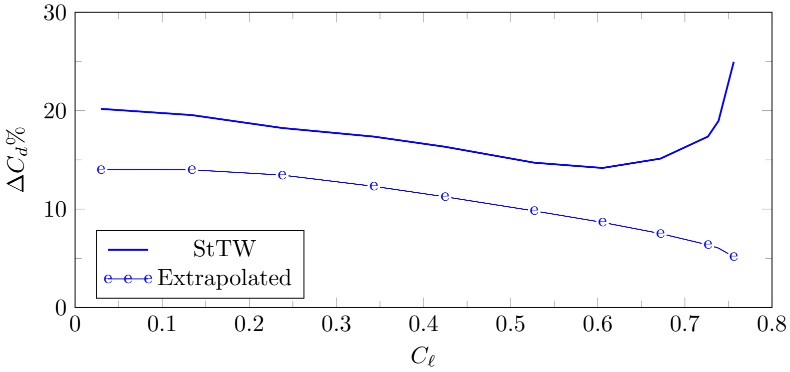

Preliminary RANS investigation

- StTW interacts with the shock-wave and the pressure field
- The overall benefits exceed the extrapolated scenario

Further investigations needed:

- The ΔB^+ computed over a flat plate has been imposed everywhere
- The interaction with the shock-wave should be reliably investigated

Outline

- Introduction
- Preliminary RANS investigation
- Incompressible DNS over a bump
- Transonic DNS over a wing slab
- Blowing actuator

Channel with a bump

- Incompressible DNS of a channel with a small bump
- Periodic + non-periodic domain
- $Re_\tau = 200$, $(L_x, L_y, L_z) = (25h, 3.2h, 2h)$, $(N_x, N_y, N_z) = (1120, 312, 241)$
- Without (Ref) and with StTW (Flat channel: $\Delta\tau \sim 45\%$)

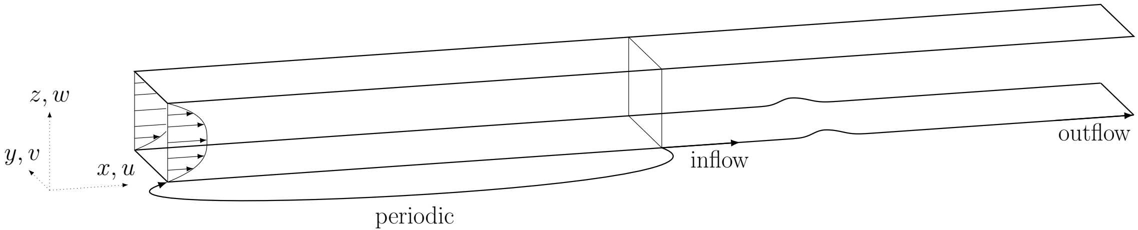

Curved wall

Two (small) bump geometries, one inducing mild separation

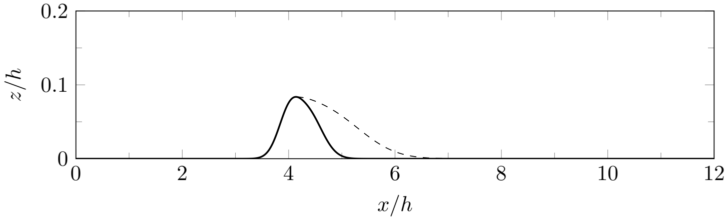

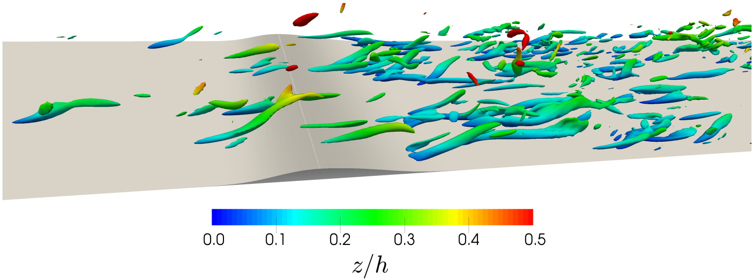

Wall shear stress

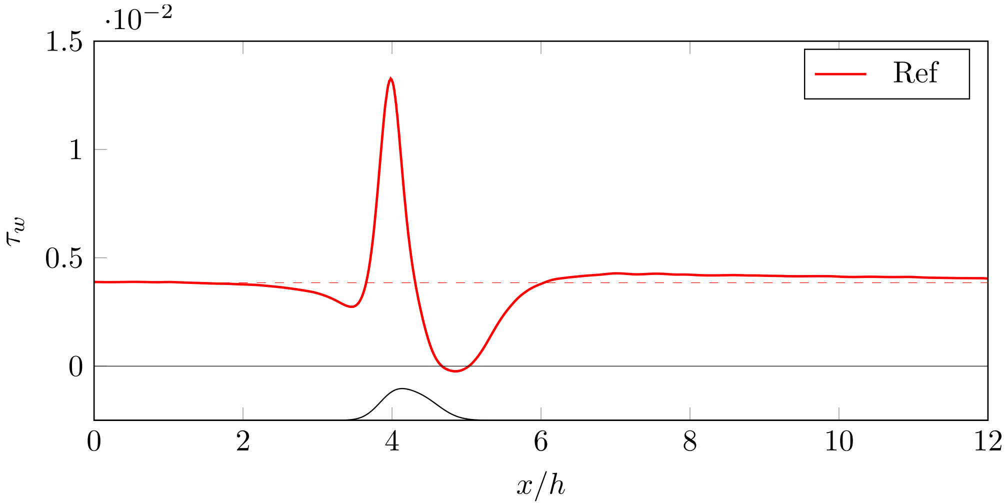

Wall shear stress

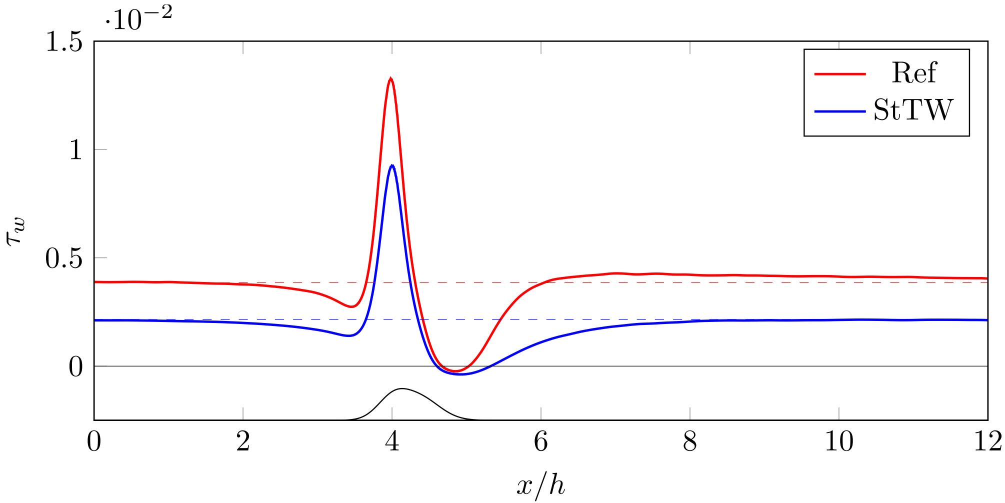

Pressure at the wall

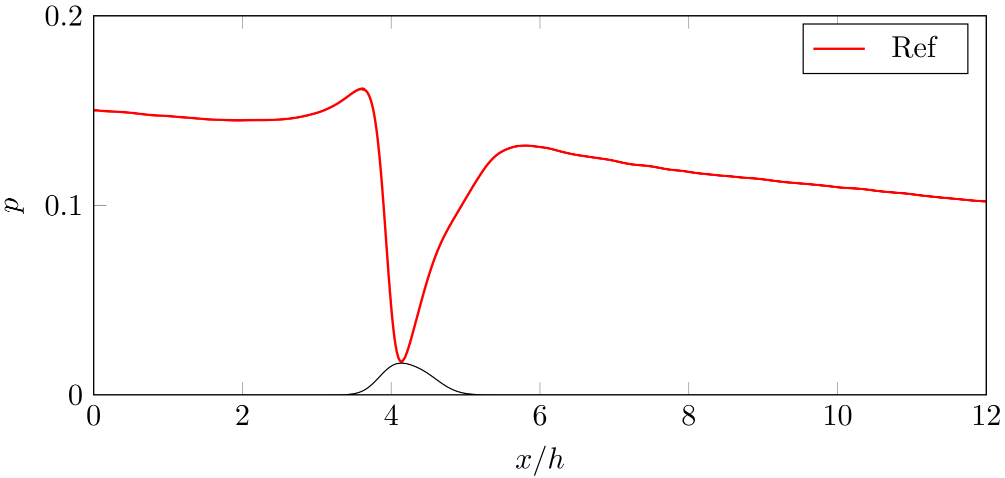

Pressure at the wall

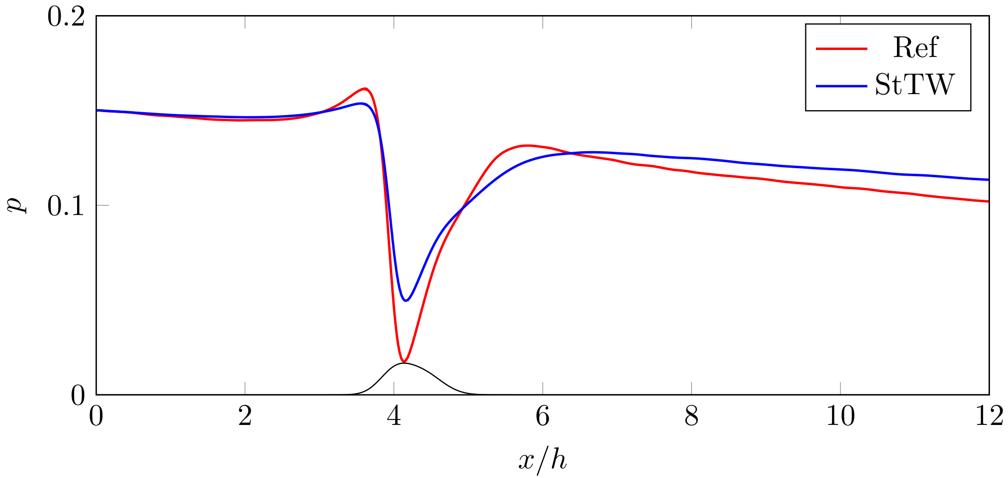

Power budget

	Plane			Bump			
	Ref	StTW	Δ	Ref	StTW	Δ	e
P_f/P_{tot}	1	0.545	$-$**45.5%**	0.918	0.462	$-$**49.6%**	-45.5%
P_p/P_{tot}	–	–	–	0.082	0.073	$\underline{-10.3\%}$	–
Net Power Savings	–		-11.5%	–		-15.3%	-10.5%

Channel with a bump

- Interaction between friction drag reduction and total drag is more complex
- Benefits of skin-friction drag reduction techniques may be underestimated

Outline

- Introduction
- Preliminary RANS investigation
- Incompressible DNS over a bump
- Transonic DNS over a wing slab
- Blowing actuator

StTW over a transonic wing slab

- Transonic DNS: $M = 0.7$, V2C airfoil, $AoA = 4$
- $Re = 3 \cdot 10^5$, $(N_x, N_y, N_z) = (4096, 256, 512)$
- Transition obtained via volume force at $x/c = 0.1$
- Without (Ref) and with StTW
- Control applied over the suction side only $0.2 < x/c < 0.8$

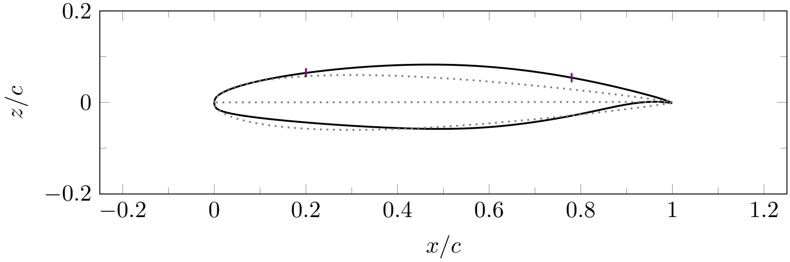

StTW over a transonic wing slab

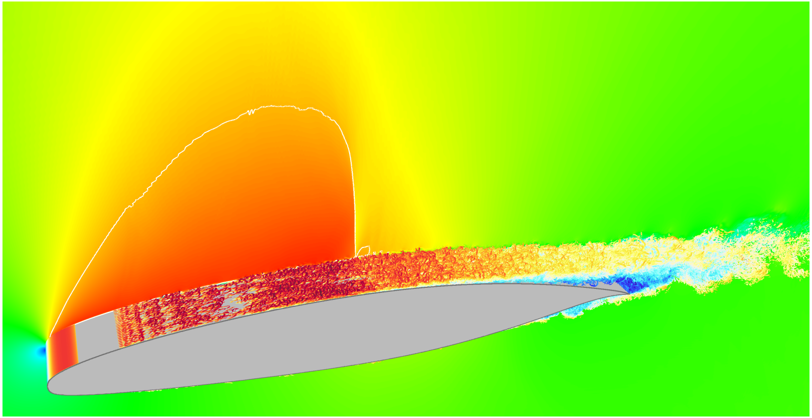

Boundary layer

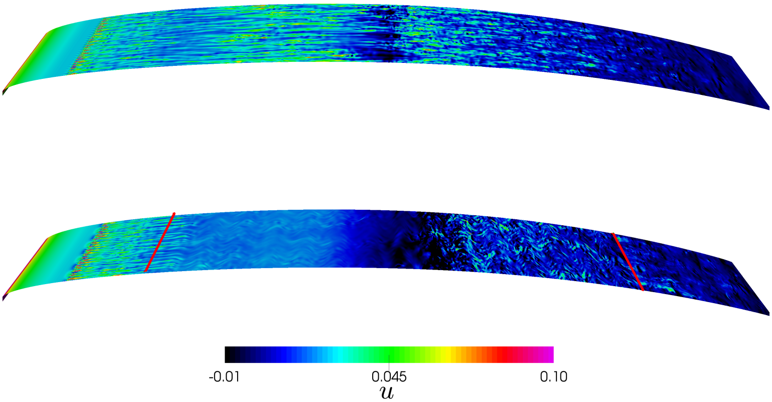

Friction coefficient

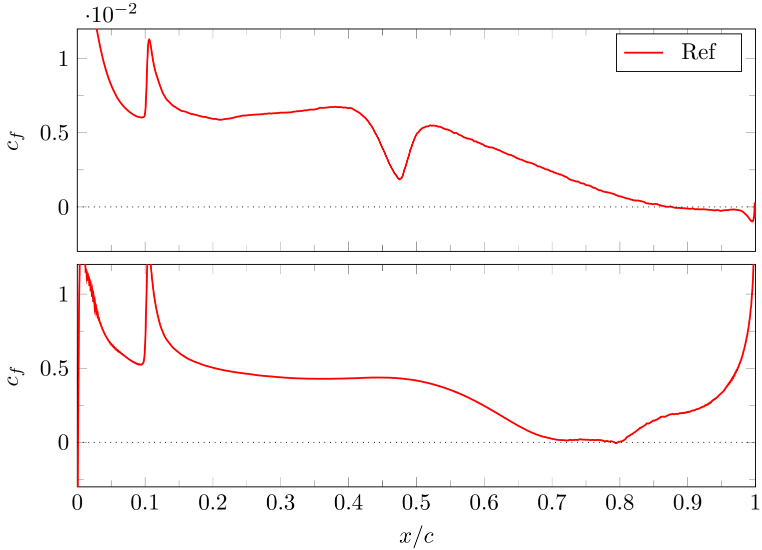

Friction coefficient

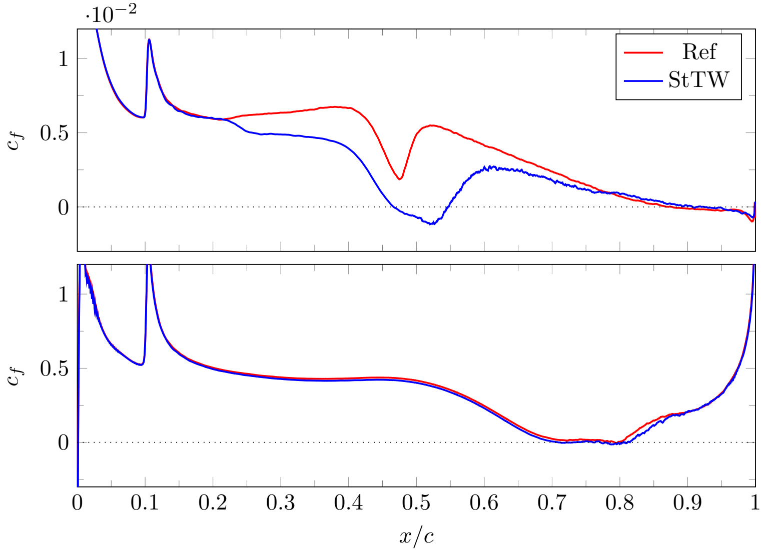

Pressure coefficient

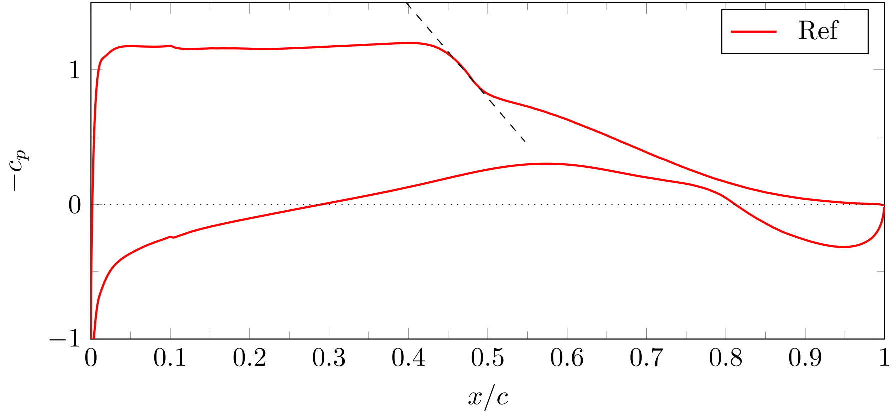

Pressure coefficient

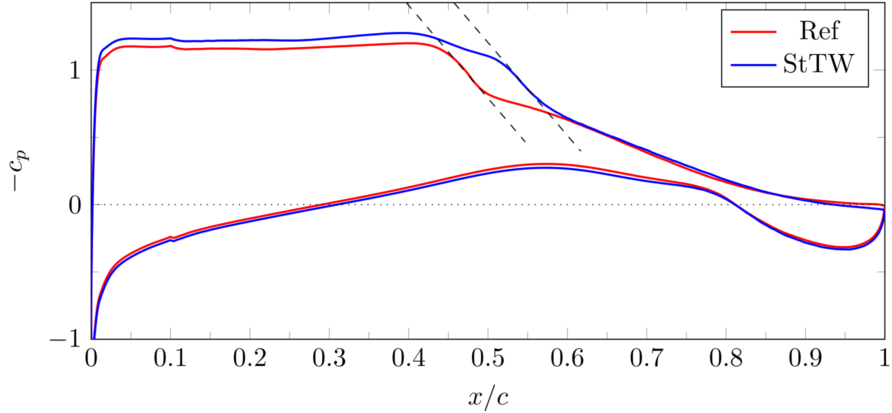

Mach distribution

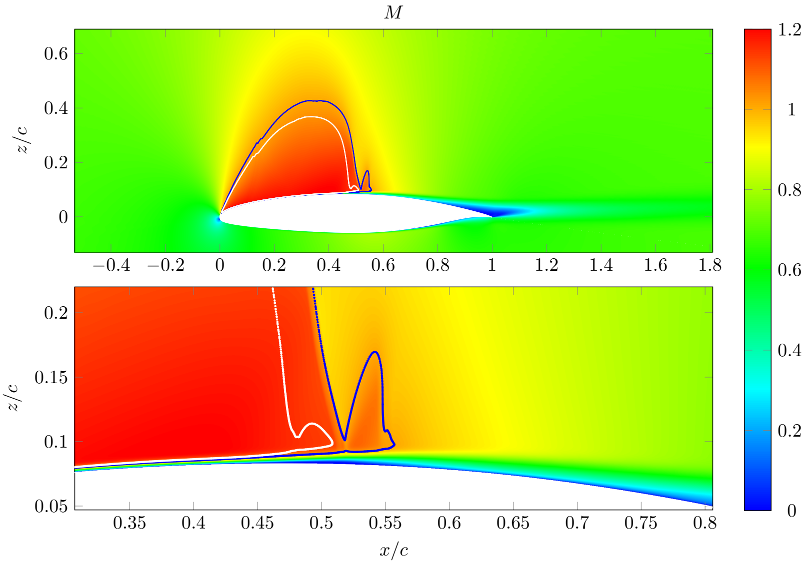

StTW over a transonic wing slab

	Ref	StTW	Δ
$C_{d,f}$	0.0084	0.0071	-15.2%
$C_{d,p}$	0.0165	0.0174	$+5.5\%$
C_d	0.0249	0.0245	-1.5%
C_ℓ	0.74	0.815	$+10.1\%$
L/D	29.7	33.3	$+11.8\%$

StTW over a transonic wing slab

	Ref	StTW	Δ	Δ at constant C_ℓ
$C_{d,f}$	0.0084	0.0071	-15.2%	
$C_{d,p}$	0.0165	0.0174	$+5.5\%$	
C_d	0.0249	0.0245	-1.5%	-11%
C_ℓ	0.74	0.815	$+10.1\%$	-
L/D	29.7	33.3	$+11.8\%$	$+11.8\%$

StTW over a transonic wing slab

	Ref	StTW	Δ	Δ at constant C_ℓ
$C_{d,f}$	0.0084	0.0071	-15.2%	
$C_{d,p}$	0.0165	0.0174	$+5.5\%$	
C_d	0.0249	0.0245	-1.5%	-11%
C_ℓ	0.74	0.815	$+10.1\%$	-
L/D	29.7	33.3	$+11.8\%$	$+11.8\%$

What about an entire aircraft?

StTW over a transonic wing slab

- StTW delays the shock-wave
- StTW in transonic regime induces a consistent lift increase
- Friction reduction strategies may be used locally to produce a global gain

Outline

- Introduction
- Preliminary RANS investigation
- Incompressible DNS over a bump
- Transonic DNS over a wing slab
- Blowing actuator

- Turbulent boundary layer experiment
- Non-uniform blowing slits
- 70% of friction reduction 33 w.u. downstream the actuator

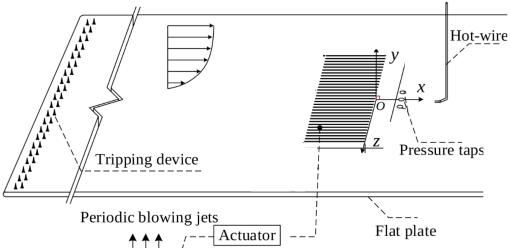

- Turbulent boundary layer experiment
- Non-uniform blowing slits
- 70% of friction reduction 33 w.u. downstream the actuator

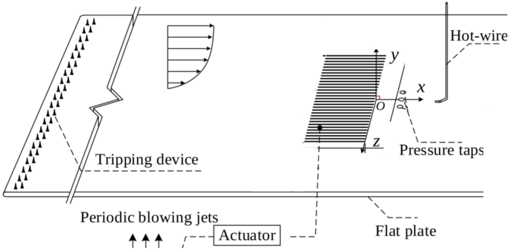

- Hypothesis: part of the friction reduction derives from streamwise vortices

Vortices produced by non-uniform blowing

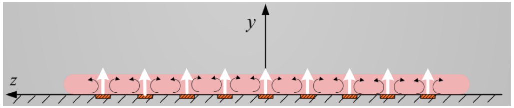

Blowing actuator - DNS

- Incompressible DNS
- Flat wall - Blowing actuator
- Uniform and non-uniform jet
- $Re_\tau = 200$, $(L_x, L_y, L_z) = (31h, 3.2h, 2h)$, $(N_x, N_y, N_z) = (1050, 384, 200)$

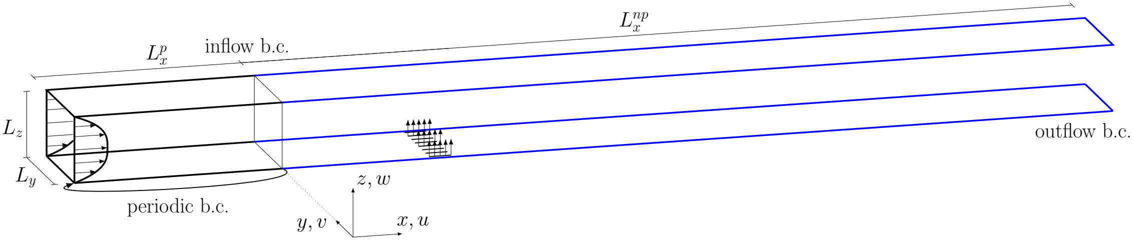

- Highly regularized streamwise vortices above the non-uniform actuator
-

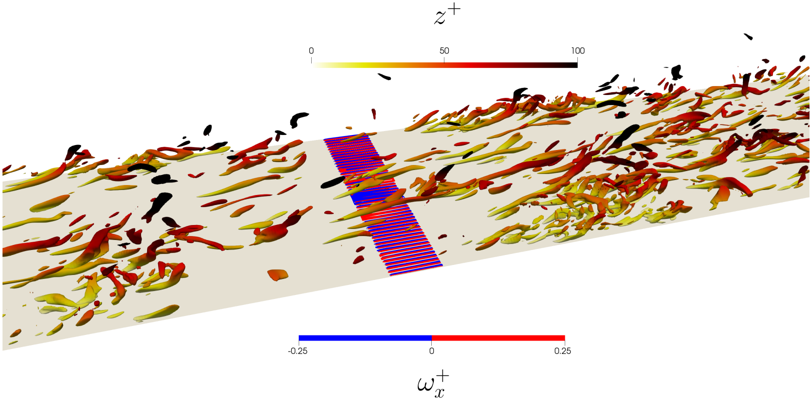

Highly regularized streamwise vortices

- Highly regularized streamwise vortices above the non-uniform actuator
- Vortices are absent over the uniform actuator

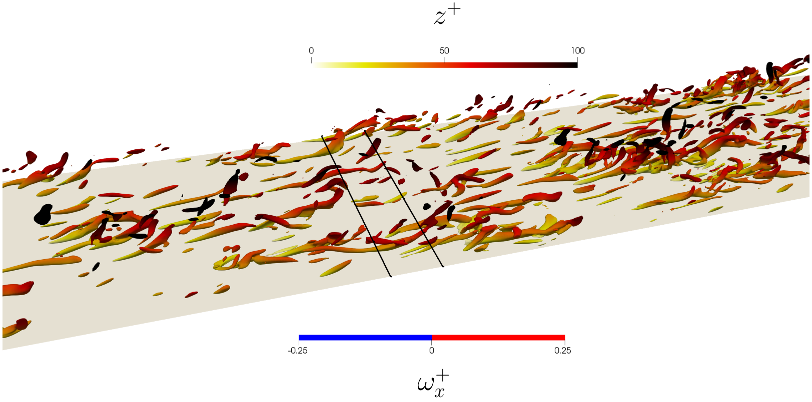

Friction coefficient

- Friction reduction close to the experimental 70%
-

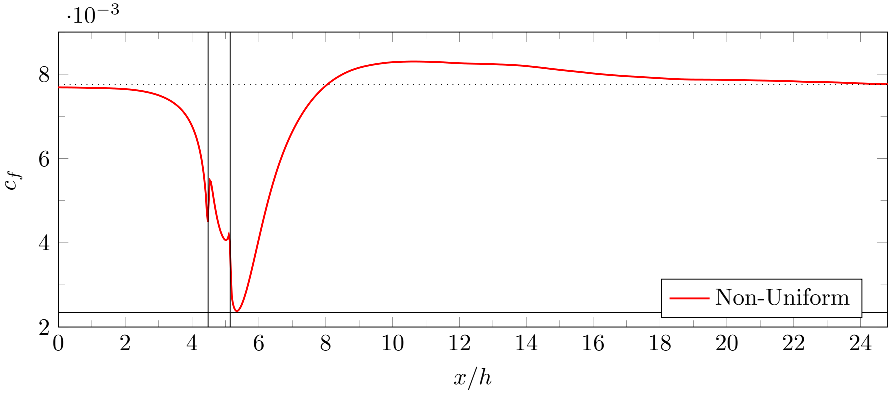

Friction coefficient

- Friction reduction close to the experimental 70%
- Negligible impact of the non-uniformity

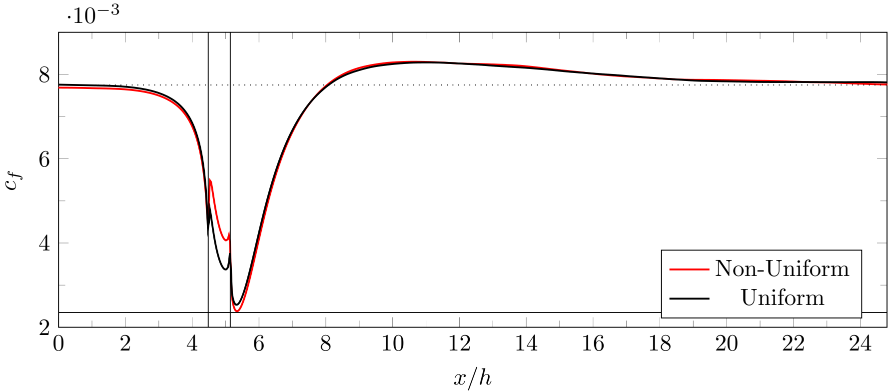

Friction coefficient

- Overall friction drag reduction around 3%
- Additive drag to slow down the air higher than 7%

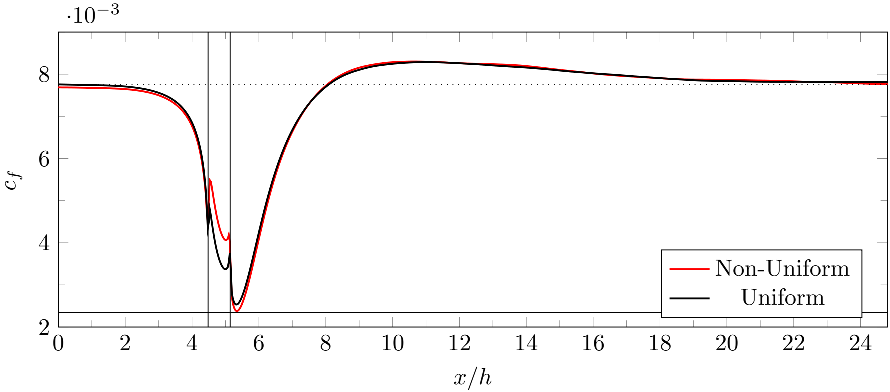

Blowing actuator - DNS

- Blowing actuator successfully reproduced via DNS
- Non-uniformity of the jet induces almost negligible effects
- Limited performances over flat walls

Conclusions

- The extrapolated answer is incorrect
- StTW interacts with pressure forces
- Friction reduction delays the shock-wave and causes lift increase
- Non-uniformity has negligible effects on blowing actuator efficiency

Conclusion

Friction reduction strategies may be thought as local actuators

whose cost is a benefit

Thank you for your attention

Questions?

Friction Prediction

When the topography modulation is shallow enough

- the response of the flow field is linear
- dimensionless shear stress perturbation $\delta\tau \ll 1$
- the problem can be addressed in $\widehat{\textit{Fourier}}$ space
- the Fourier-transformed $\widehat{\delta\tau}$ is proportional to $\widehat{h}$ via:

$$T(k^+) = \frac{\widehat{\delta\tau_{dim}/\tau_{dim}}}{dh_{dim}/\widehat{dx_{dim}}} = \frac{\widehat{\delta\tau}}{-ik\widehat{h}}$$

Friction prediction over a bump

- Incompressible DNS of a channel with a small bump
- Laminar & turbulent
- DNS & analytical prediction
- $Re_\tau = 200$, $(L_x, L_y, L_z) = (25h, 3.2h, 2h)$, $(N_x, N_y, N_z) = (1120, 1/312, 241)$

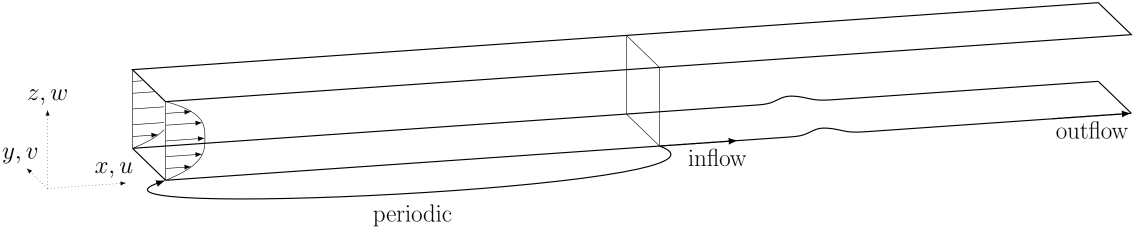

Laminar

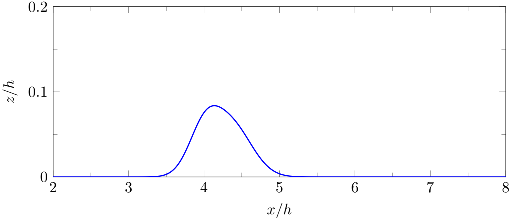

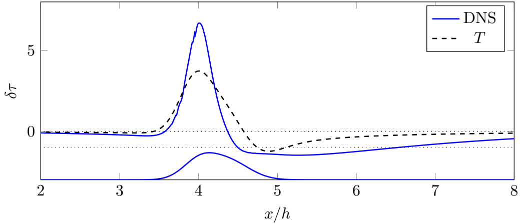

Laminar

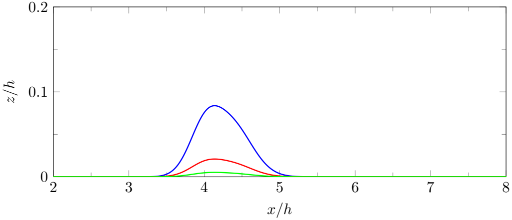

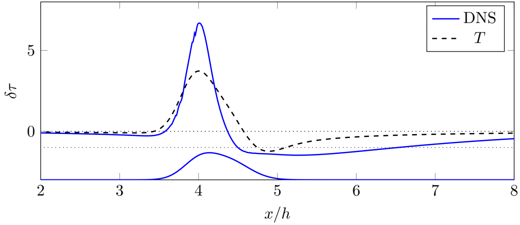

Laminar

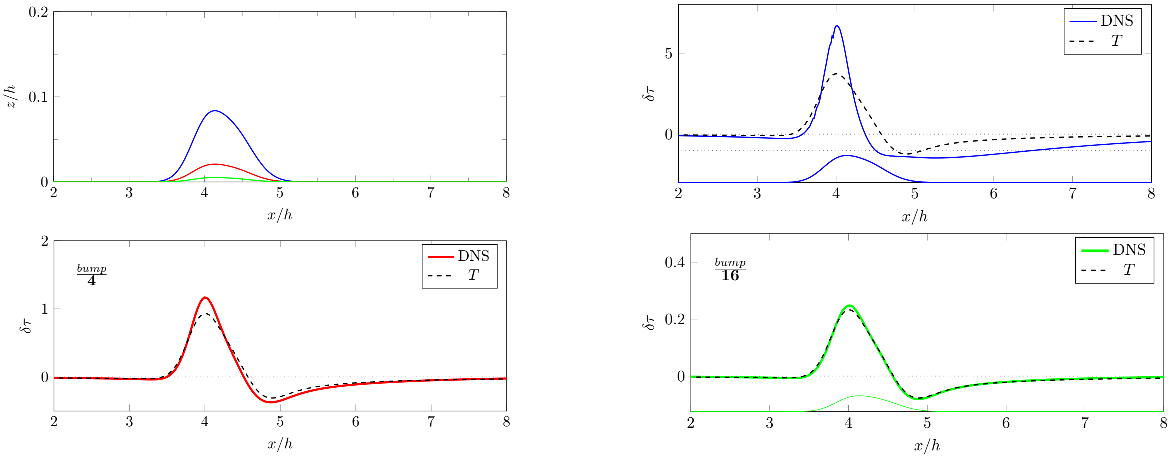

0.2
0.1
0
z/h
2 3 4 5 6 7 8
x/h
DNS
T
5
0
$\delta\tau$
2 3 4 5 6 7 8
x/h
2
1
0
$\delta\tau$
$\frac{bump}{\mathbf{4}}$
DNS
T
2 3 4 5 6 7 8
x/h
0.4
0.2
0
$\delta\tau$
$\frac{bump}{\mathbf{16}}$
DNS
T
2 3 4 5 6 7 8
x/h

Turbulent

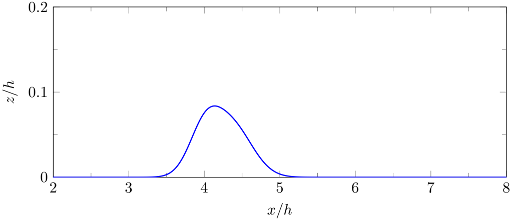

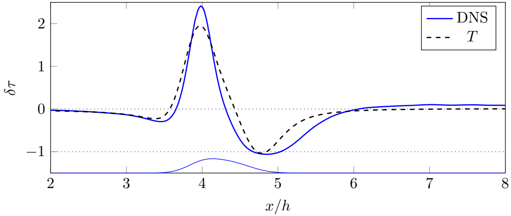

Turbulent

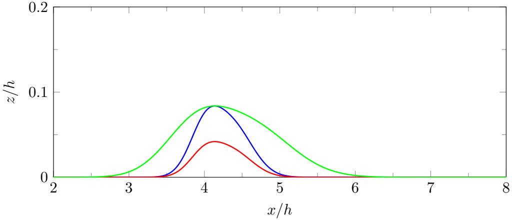

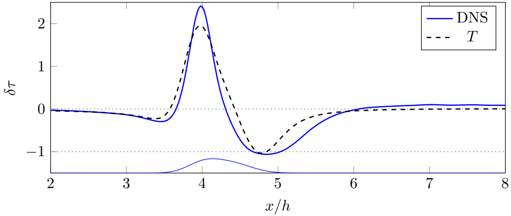

Turbulent

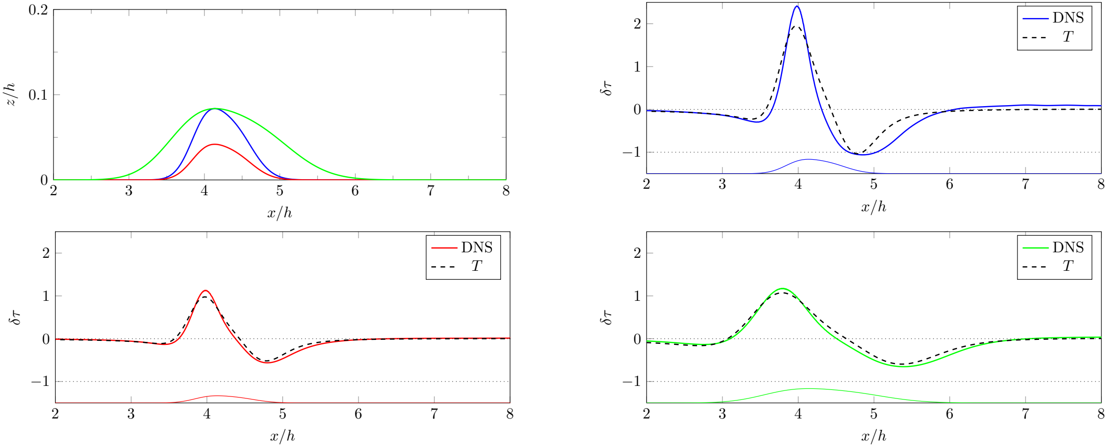

Friction Prediction

- A good agreement is present in both laminar and turbulent regime
- The qualitative behavior is confirmed even when linearity range is strongly exceeded
- By reducing the bump size friction prediction approaches numerical data

Introduction

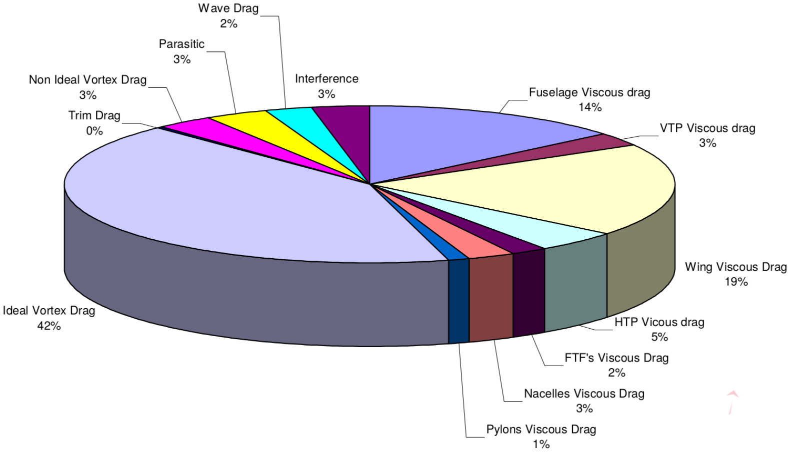

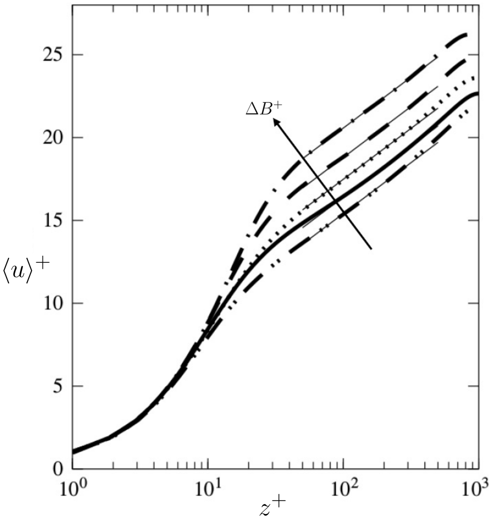
25
20
15
10
5
0
ΔB^+
$\langle u \rangle^+$
10^0
10^1
10^2
10^3
z^+

Introduction

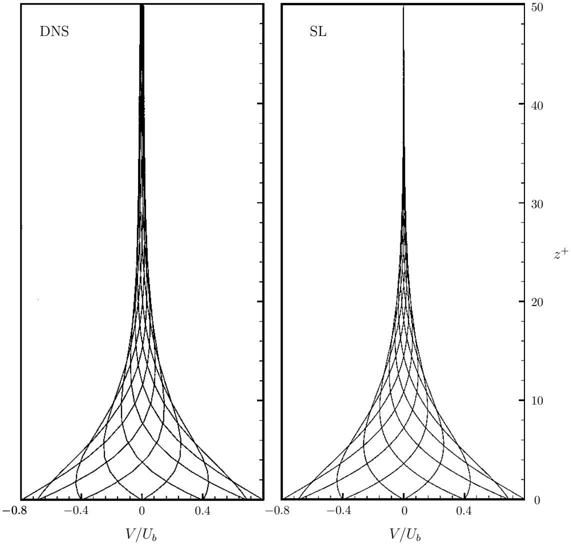

Background (Gatti & Quadrio, *JFM*16)

Waves can be assimilated to drag-reducing roughness

- Streamwise travelling waves produce a vertical shift ΔB of the logarithmic portion of the mean velocity profile

$$U^+ = \frac{1}{\kappa}\log(y^+) + B + \Delta B^+$$

- Drag reduction rate R is linked to ΔB

$$\Delta B^+ = \sqrt{\frac{2}{C_{f,0}}}\left[(1-\mathcal{R})^{-1/2} - 1\right] - \frac{1}{2\kappa}\ln(1-\mathcal{R}).$$

- Achievable friction reduction at flight-$Re > 20\%$

Background (Gatti & Quadrio, *JFM*16)

Waves can be assimilated to drag-reducing roughness

- Streamwise travelling waves produce a vertical shift ΔB of the logarithmic portion of the mean velocity profile

$$U^+ = \frac{1}{\kappa}\log(y^+) + B + \Delta B^+$$

- Drag reduction rate R is linked to ΔB

$$\Delta B^+ = \sqrt{\frac{2}{C_{f,0}}}[(1-\mathcal{R})^{-1/2} - 1] - \frac{1}{2\kappa}\ln(1-\mathcal{R}).$$

- Achievable friction reduction at flight-Re > 20%

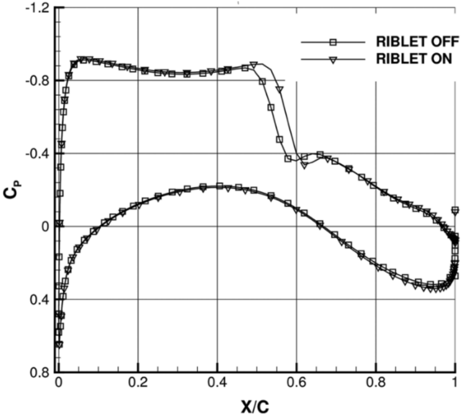

Figure 2.1: *Comparison of the pressure coefficient, with and without riblets, over a wing section of the CRM aircraft. Here, x/c is the non-dimensional chord-wise coordinate and c_p is the pressure coefficient. Taken from Mele, Tognaccini, and Catalano (2016).*

DLR-F6 is a modern transport aircraft, with a **transonic design**

- RANS: Spalart-Allmars model, fully turbulent boundary layer
- Coarse mesh from in Drag Prediction Workshop website
- $Re = 3 \cdot 10^6$ based on reference chord
- $M = 0.75$
- Forcing is introduced by a modified wall function
- Forcing applied over the entire aircraft

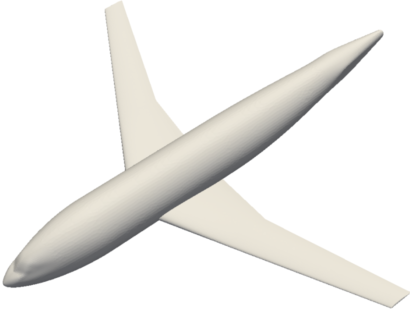

Computational domain

Coarse mesh from the 2nd Drag Prediction Workshop
$2 \cdot 10^6$ cells, 61% tethraedals and 39 % prisms.

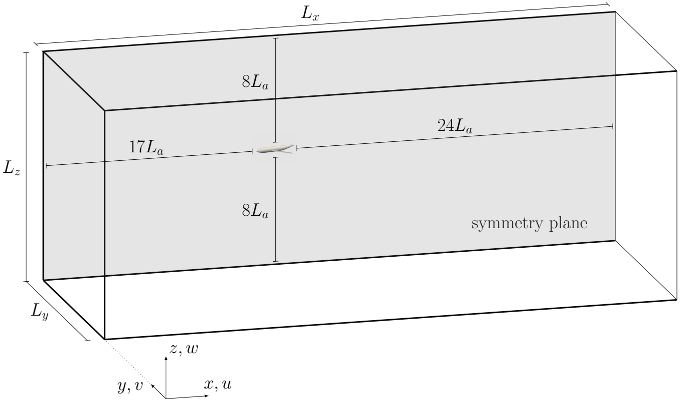

AeroX

A GPU-CPU compressible RANS solver

- Finite volumes
- Compressible (transonic)
- Speedup by GPU:

(2015)	AMD 380X $\sim 230 USD$	AMD FURY X $\sim 650 USD$
i7 5930k-6 $\sim 600 USD$	$4.3x$	$8.7x$

In the present work:

- GPU: AMD 380X
- $2 \cdot 10^6$ elements: convergence in $\sim$ 45 min

Validation

DLR-F6 Polar curve

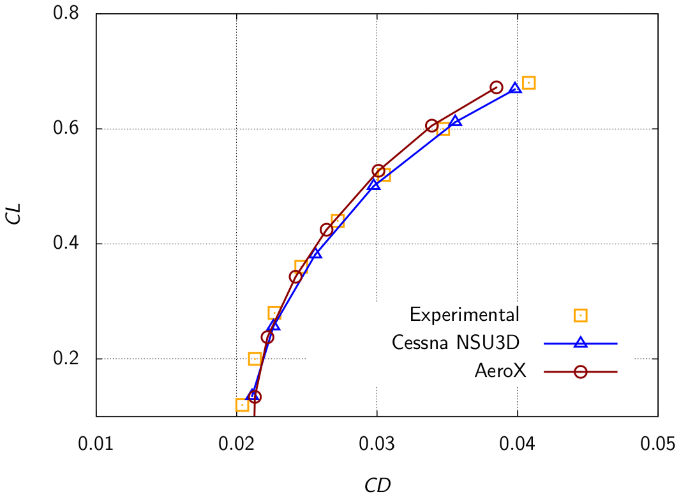

Aircraft drag reduction

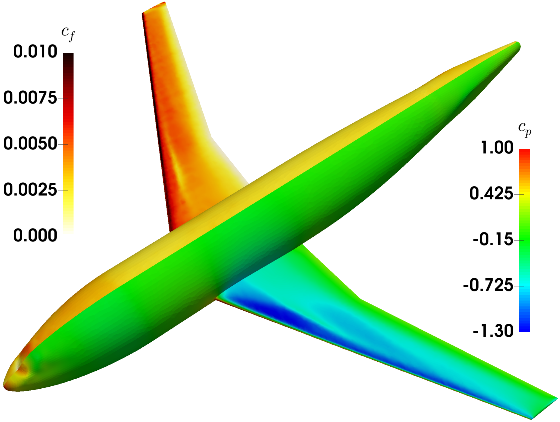

Aircraft drag reduction

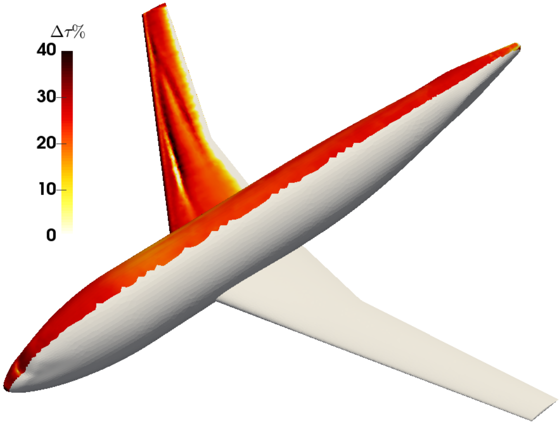

Aircraft drag reduction

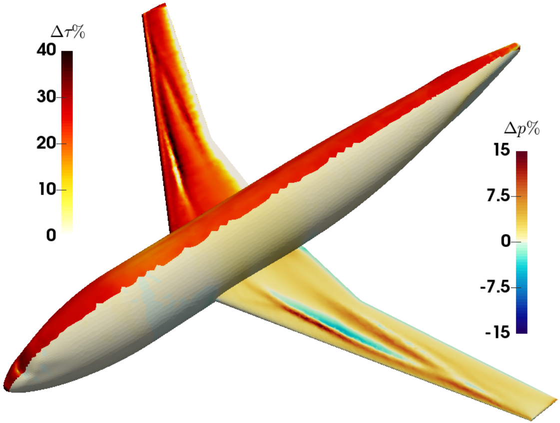

Aircraft drag reduction

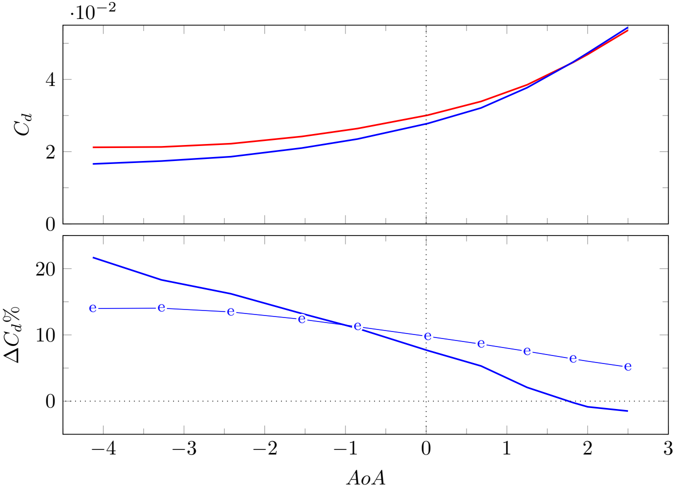

Comparison of drag coefficients as a function of AoA. First panel: reference (red) and controlled (blue) C_d; second panel: computed $\Delta C_d\%$ (thick line) compared with the extrapolated one (thin line with symbols).

Aircraft drag reduction

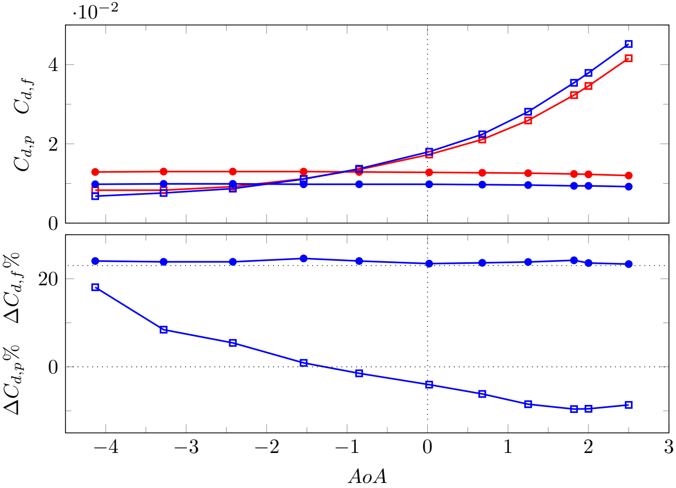

Pressure (lines with squares) and friction (lines with circles) drag components. Top: reference (red) and controlled (blue) cases; bottom: pressure and friction drag reduction $\Delta C_{d,p}$ and $\Delta C_{d,f}$, respectively.

Aircraft drag reduction

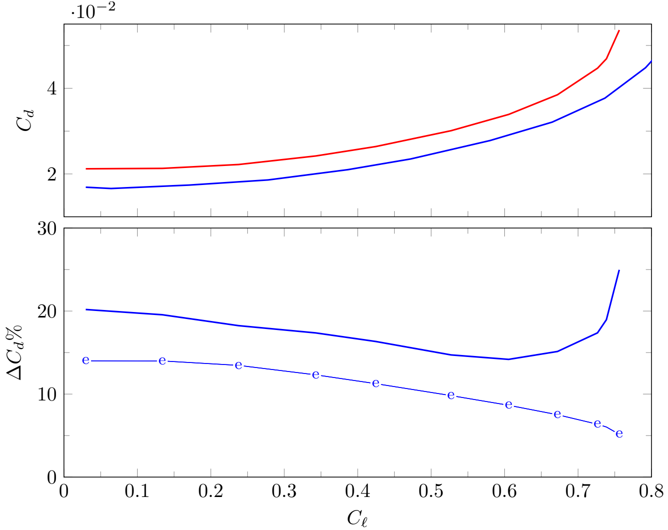

Comparison of drag coefficients as a function of C_ℓ. Top reference (red) and controlled (blue) C_d; bottom: computed $\Delta C_d\%$ compared with the extrapolated one (thin line with symbols).

Aircraft drag reduction

	Ref	StTW	Δ	e
$C_{d,f}$	0.013	0.010	-23.4%	-23%
$C_{d,p}$	0.017	0.018	$+4.0\%$	-
C_d	0.030	0.028	-7.6%	-10%
C_ℓ	0.52	0.57	$+10.1\%$	-
L/D	17.5	20.9	$+19.2\%$	$+11.1\%$

Table: Force coefficients. Here, $C_{d,f}$ and $C_{d,p}$ are the friction and pressure components respectively, with $C_d = C_{d,f} + C_{d,p}$. C_ℓ is the lift coefficient, while L/D represents the lift/drag ratio.

Aircraft drag reduction

Breguet Range Equation:

$$Range = \frac{U_\infty}{g\ SFC} \ln\left(\frac{\mathcal{W}_{initial}}{\mathcal{W}_{final}}\right) \frac{L}{D}$$

Aircraft drag reduction

- P_{net} is supposed to decrease, over a flat plate, as fast as $\Delta\tau$
- P_{req} is supposed to be 13% of the power spent due to friction drag in Ref.

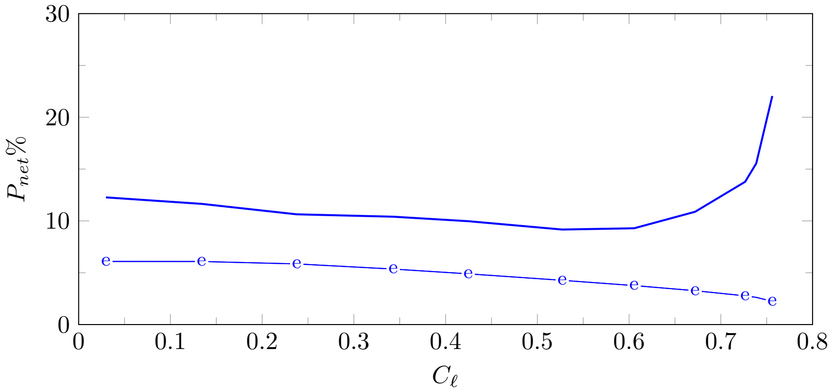

Comparison with MTC 2016

Despite the differences

	MTC16	Actual
Solver	UZEN / FLOWer	AeroX
Aircraft	CRM	DLR-F6
Re	$5 \cdot 10^6$	$3 \cdot 10^6$
M	0.85	0.75
Turbulence model	SST	Spalart-Allmaras
DR technique	Riblets	Spanwise forcing
Forcing formulation	ω at wall	Wall function

Same qualitative results:

- Direct effects: R close to the expected value;
- Indirect effects: Shock delay - Lift increase;

Channel with a bump

- Incompressible DNS, primitive variables, staggered grid
- Second-order FD, implicit immersed boundary
- Fractional time-stepping method using a third-order Runge-Kutta scheme
- The Poisson equation for the pressure is solved by an iterative SOR algorithm
- $Re_\tau = 200$, $(L_x, L_y, L_z) = (25h, 3.2h, 2h)$, $(N_x, N_y, N_z) = (1120, 312, 241)$
- Outflow condition

$$\frac{\partial u_i}{\partial t} + U_c \frac{\partial u_i}{\partial x} = 0, \qquad i = 1, 2, 3$$

- CFR with mean CFL ~ 0.5; T=1000; $T^+ \sim 12000$; $\Delta t = 1.5 \cdot 10^{-3}$

Channel with a bump

- $Re_\tau = 200$, $(L_x, L_y, L_z) = (25h, 3.2h, 2h)$, $(N_x, N_y, N_z) = (1120, 312, 241)$

Periodic

- $(L_x, L_y, L_z) = (4\pi h, \pi h, 2h)$
- $(N_x, N_y, N_z) = (320, 312, 241)$
- $(\Delta x^+, \Delta y^+, \Delta z^+_{lower}, \Delta z^+_{centre}, \Delta z^+_{upper}) = (8, 2, 0.2, 4, 0.8)$

Non-Periodic

- $(L_x, L_y, L_z) = (12h, \pi h, 2h)$
- $(N_x, N_y, N_z) = (800, 312, 241)$
- $(\Delta x^+_{min}, \Delta x^+_{max}, \Delta y^+, \Delta z^+_{lower}, \Delta z^+_{centre}, \Delta z^+_{upper}) = (1, 8, 2, 0.2, 4, 0.8)$

Two (small) bump geometries, one inducing mild separation

$$G_1(x) = a \exp\left[-\left(\frac{x-b}{c}\right)^2\right] + a' \exp\left[-\left(\frac{x-b'}{c'}\right)^2\right].$$

- $a = 0.0505$, $b = 4$, $c = 0.2922$, $a' = 0.060425$, $b' = 4.36$, $c' = 0.3847$; $h_b = 0.0837$
- G_2 is identical up to the tip; streamwise expansion factor of 2.5 to the rear part

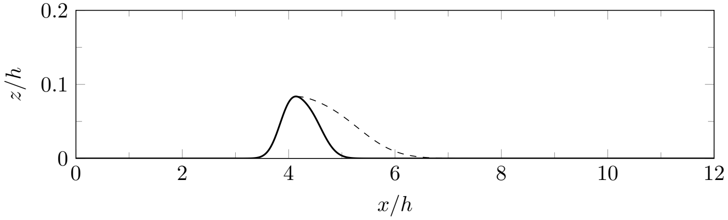

Spanwise forcing

- $A = 0.75$, $A^{+} = 12$
- $\omega = \pi/10$ and $\kappa_x = 2$

$$V_w(x, t) = A \sin\left(\kappa_x x - \omega t\right).$$

Streamwise velocity

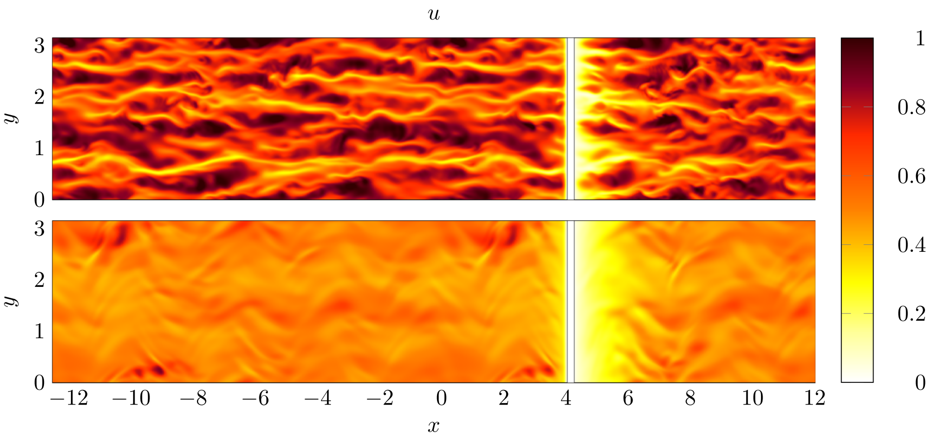

Colour plot of an instantaneous streamwise velocity field, in the plane $z = 0.08$ over the bump G_1, for the reference case (top) and with StTW (bottom). Flow is from left to right, and the upstream periodic section ends at $x = 0$.

Spanwise velocity

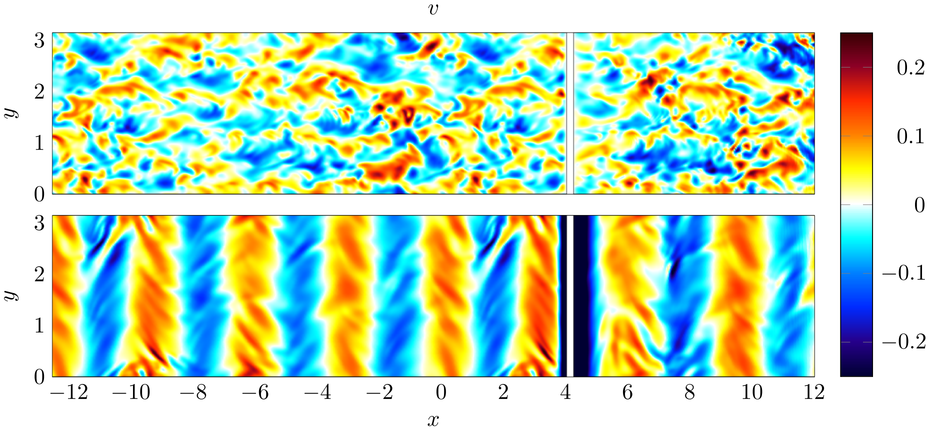

Colour plot of an instantaneous spanwise velocity field, in the plane $z = 0.08$ over the bump G_1.

mean wall-normal velocity

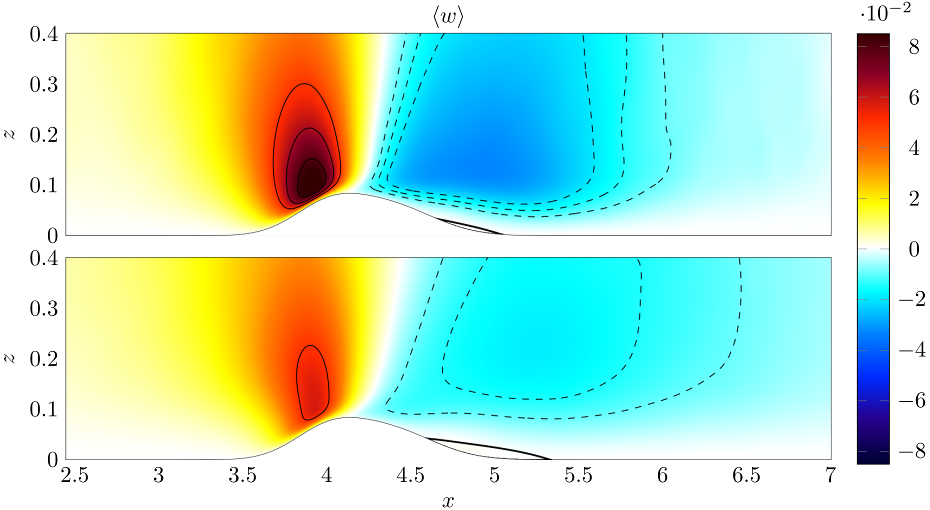

Colour plot of the mean vertical velocity w for the bump G_1: top, reference case; bottom, StTW. Positive contours (continuous lines) are drawn for $w = (0.05, 0.065, 0.08)$, and negative contours (dashed lines) are drawn for $w = (-0.02, -0.015, -0.01)$. The thick black line indicates $u = 0$ and marks the boundary of the separated region.

Mean pressure

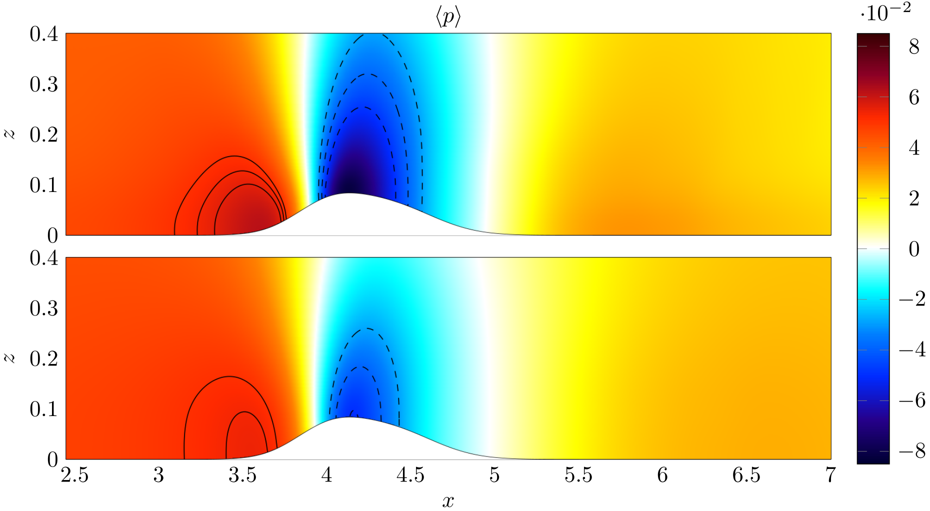

Colour map of the mean pressure p for the bump $G_{\mathbf{1}}$: top, reference case; bottom, StTW. Positive contours (continuous lines) are drawn for $p = (0.05, 0.0525, 0.055)$, and negative contours (dashed lines) are drawn for $p = (-0.05, -0.04, -0.03)$.

Coefficients

$$c_f(x) = \frac{2\tau(x)}{\rho U_b^2}, \qquad c_p(x) = \frac{2p(x)}{\rho U_b^2}$$

$$r(x) = 1 - \frac{c_f(x)}{c_{f,0}(x)}, \qquad \Delta c_p(x) = c_p(x) - c_{p,0}(x).$$

$$C_{d,f}^d = \frac{2}{\rho U_b^2 \ L_x} \ \hat{x} \cdot \int_0^{L_x} \mu \left(\nabla u + \nabla u^T \right) \cdot n \ \ell; \qquad C_{d,p}^d = \frac{2}{\rho U_b^2 \ L_x} \ \hat{x} \cdot \int_0^{L_x} pn \ \ell,$$

$$C_{d,f}^c = \frac{L_x^{np}}{h_b} \left(\widetilde{C}_{d,f}^d - \overline{C}_{d,f}^d \right); \qquad C_{d,p}^c = \frac{L_x^{np}}{h_b} \left(\widetilde{C}_{d,p}^d - \overline{C}_{d,p}^d \right),$$

$$\Delta c_d(x) = c_{d,0}(x) - c_d(x), \qquad R(x) = \frac{\int_0^x \Delta c_d(x')x'}{\int_0^{L_x} c_{d,0}(x')x'}$$

Friction reduction

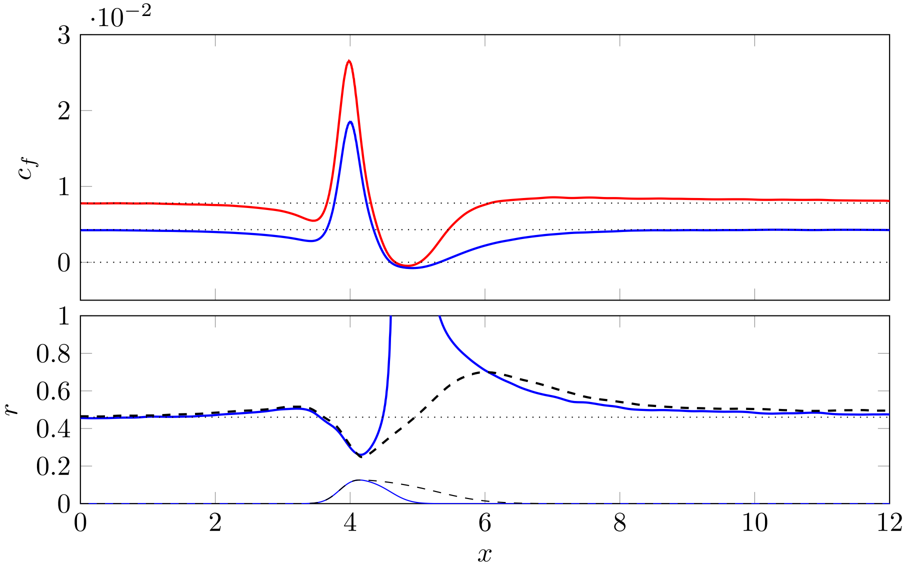

Wall shear stress

$$R(x) = \frac{\tau_w(x)^{Ref} - \tau_w(x)^{StTW}}{\tau_w(x)^{Ref}}$$

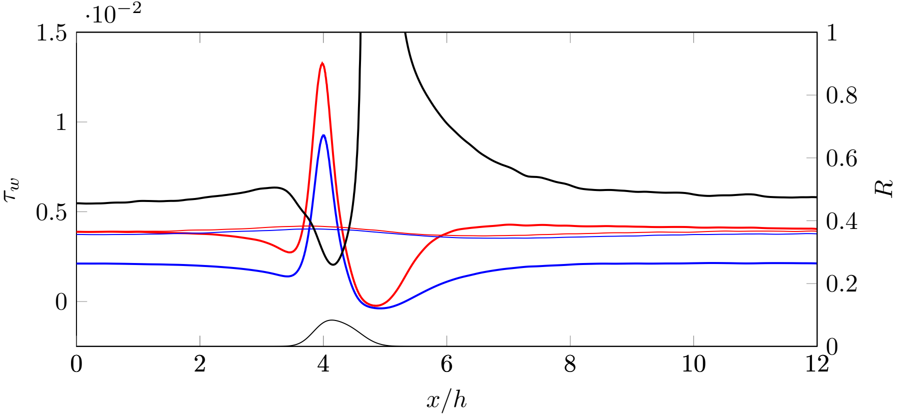

Pressure changes

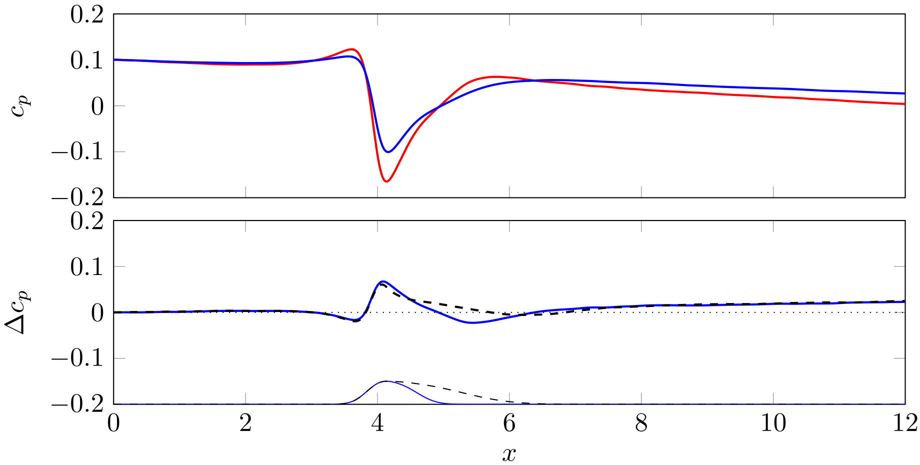

Pressure distribution $c_p(x)$ over the wall with the bump. Top: comparison between the reference case (red) and the controlled case (blue) for bump G_1. Bottom: local difference between pressure coefficients $\Delta c_p(x) = c_p(x) - c_{p,0}(x)$ for G_1 (blue) and G_2 (black dashed). The thin profiles at the bottom of the plots draw the two bumps, in arbitrary vertical units.

Lossess G_1

	Distributed losses			Concentrated losses		
	Ref	StTW	Δ	Ref	StTW	Δ
$C_{d,f} \times 10^{-2}$	0.777	0.424	-45.5%	-0.004	-4.671	
$C_{d,p} \times 10^{-2}$	0	0	0	9.891	8.887	-10.3%
$C_d \times 10^{-2}$	0.777	0.424	-45.5%	9.887	4.197	-57.5%

Table: Drag coefficients for the bump G_1. Here $C_{d,f}$ and $C_{d,p}$ are the friction and pressure components respectively, with $C_d = C_{d,f} + C_{d,p}$. Figures are for the lower wall only.

	Distributed losses			Concentrated losses		
	Ref	StTW	Δ	Ref	StTW	Δ
$C_{d,f} \times 10^{-2}$	0.781	0.418	-46.5%	-0.158	-2.904	
$C_{d,p} \times 10^{-2}$	0	0	0	7.083	6.843	-3.4%
$C_d \times 10^{-2}$	0.781	0.418	-46.5%	6.925	3.940	-43.1%

Table: Drag coefficients for the bump G_2.

Friction drag reduction

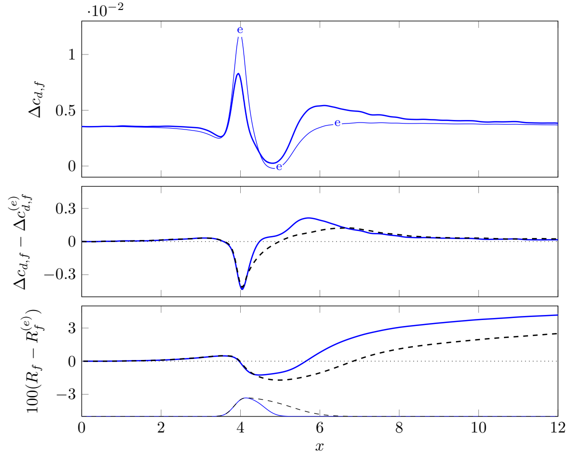

Changes in the skin-friction component of the total drag. Top: the computed $\Delta c_{d,f}$ (thick line) compared with the extrapolated $\Delta c_{d,f}^{(e)}$ (thin line with labels) for bump G_1. Center: difference between computed and extrapolated friction drag reduction, for geometries G_1 (blue line) and G_2 (black dashed line). Bottom: difference between actual R_f and extrapolated integral budget $R_f^{(e)}$ for both geometries. The thin profiles at the bottom of the plot draw the two bumps, in arbitrary vertical units.

TKE (left) and TKE production (right)

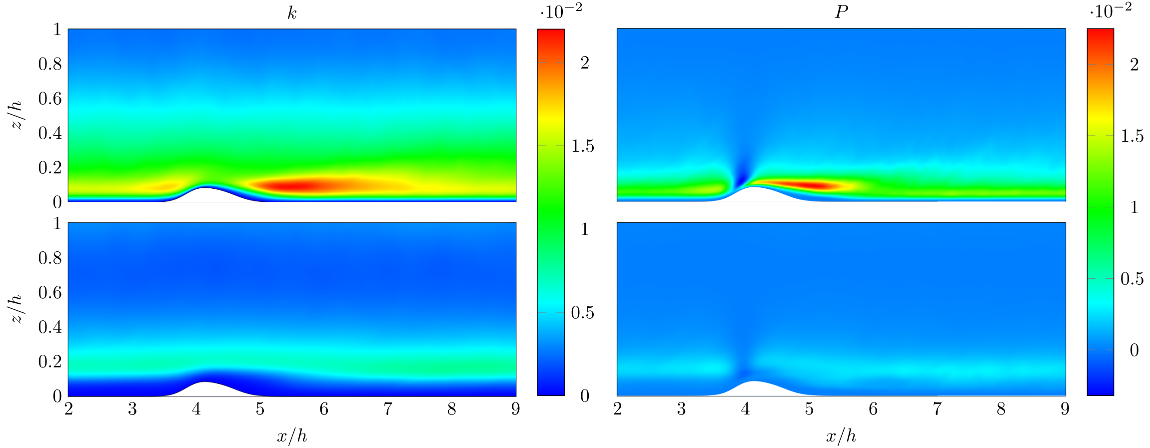

Pressure drag reduction

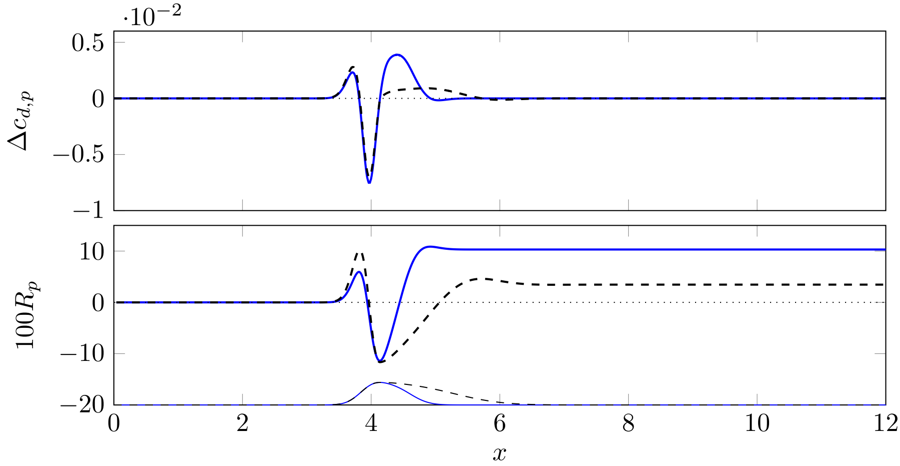

Comparison of the contribution to pressure drag changes between G_1 (blue) and G_2 (black dashed). Top: $\Delta c_{d,p}(x)$; bottom: integral budget R_p for both geometries. The thin profiles at the bottom of the plot draw the two bump geometries.

The separation bubble

Probability γ_u of a non-reversed flow:

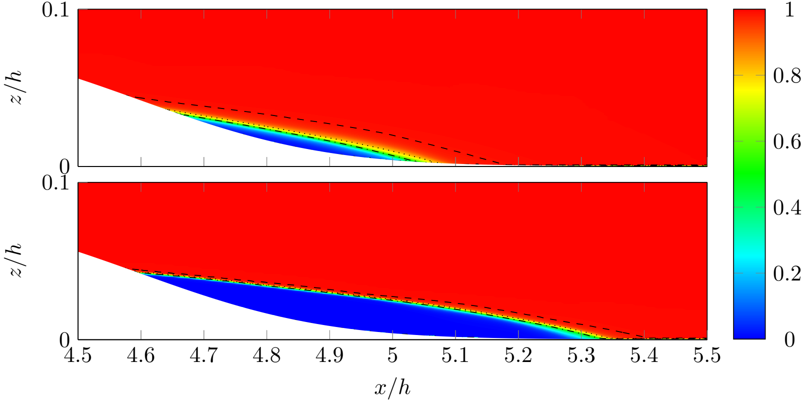

Recirculation:

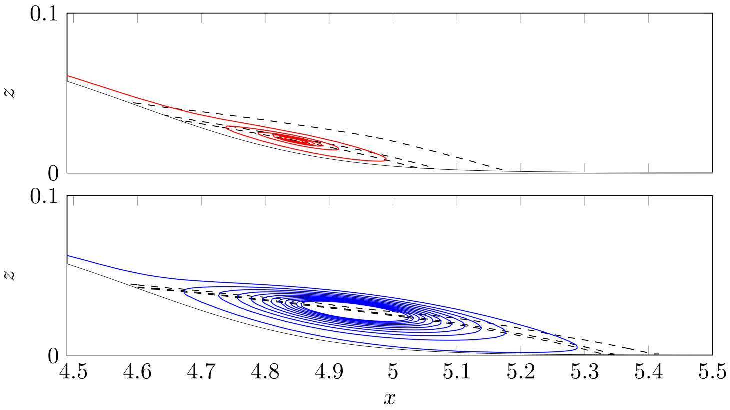

The separation bubble

	$x_{d,0}$	x_d	$x_{r,0}$	x_r	$L_{b,0}$	L_b
$\tau = 0$	4.67	4.60	5.03	5.32	0.36	0.72
$\gamma_u = 0.5$	4.65	4.59	5.04	5.33	0.39	0.74
$\gamma_u = 0.80$	4.64	4.59	5.06	5.34	0.42	0.75
$\gamma_u = 0.99$	4.58	4.58	5.18	5.40	0.60	0.82

Table: Detachment and reattachment points for the reference and controlled cases, along with longitudinal extent deduced for specified values of the probability function γ_u.

The mean velocity profile (no bump)

The maximum velocity shifts towards the actuated side and produces 4% additional drag reduction on the unactuated side!

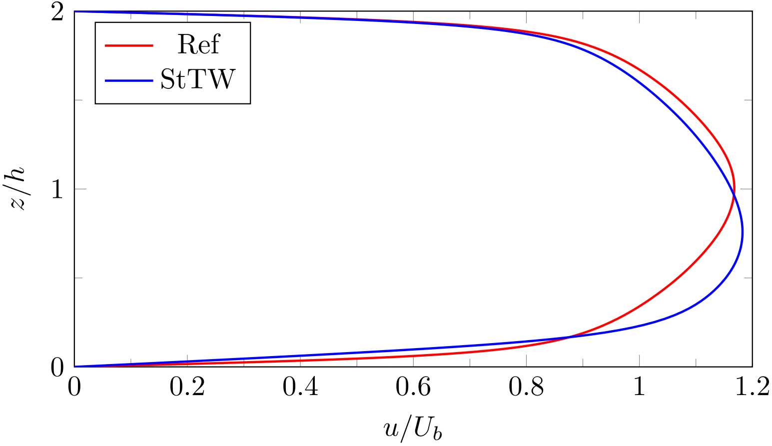

Power budget - Second Geometry

	Plane			Bump		
	Ref	StTW	Δ	Ref	StTW	Δ
P_f/P_{tot}	1	0.535	$-\mathbf{46.5\%}$	0.948	0.480	$-\mathbf{49.0\%}$
P_p/P_{tot}	—	—	—	0.060	0.058	-3.4%
Net Power Savings	—		-12.5%	—		-15.1%

Transonic DNS

- Finite volumes, second order
- Ducros sensor to third-order weighted essentially non-oscillatory (WENO) near discontinuities
- Far-field numerical boundary conditions rely on characteristic decomposition
- Third-order Runge-Kutta algorithm

Computational Mesh

$$(L_x,\ L_y,\ L_z) = (100,\ 0.1,\ 100);\ (n_x, n_y, n_z) = (4096, 256, 512)$$

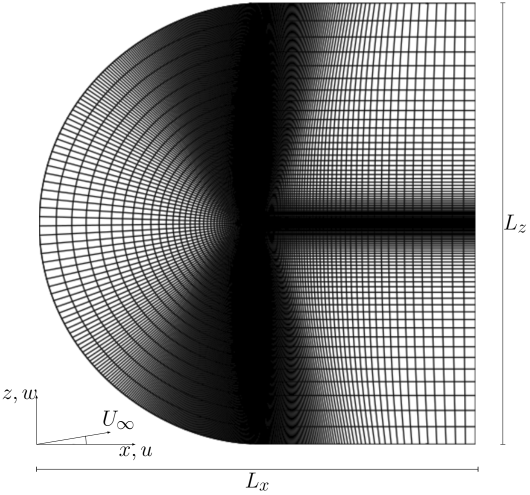

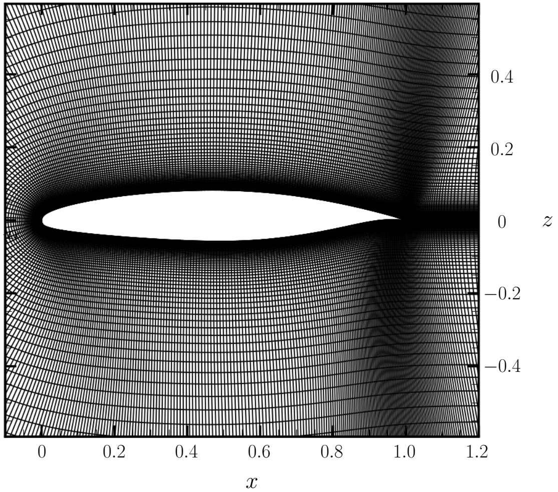

Spanwise forcing

$$V_w(x,t) = A \sin\left(\kappa_x x - \omega t\right).$$

- u'_τ taken from $x = 0.2$ to $x = 0.4$ in the reference case
- $A = 0.684$, $A^+ = 12$
- $\omega = 11.3$, $\omega^+ = 0.06$
- $\kappa_x = 161$, $\kappa_x^+ = 0.013$

Instantaneous flow field

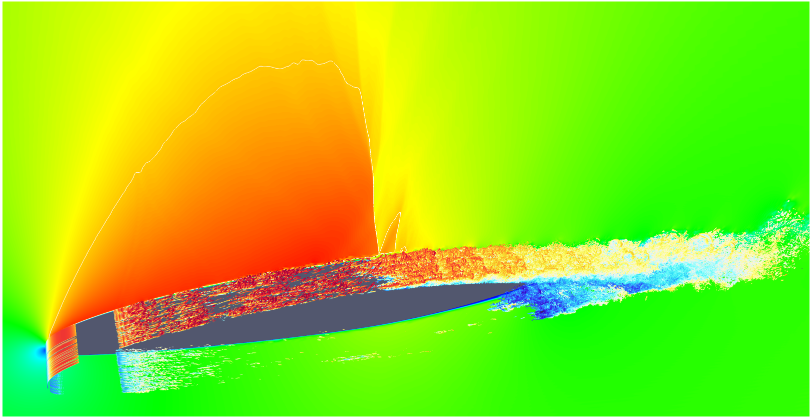

Pressure distribution

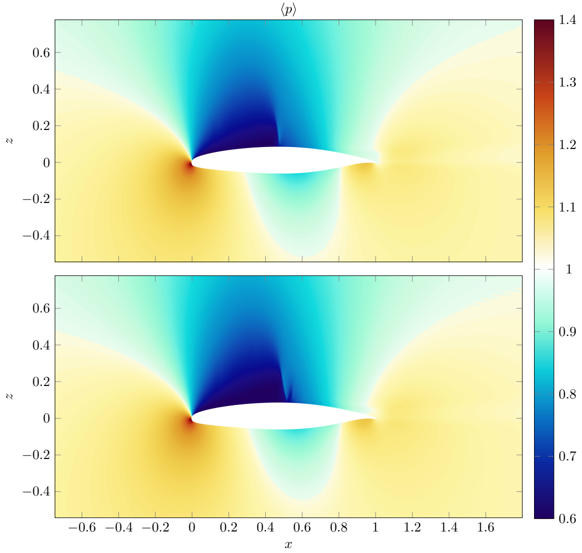

Numerical Schlieren

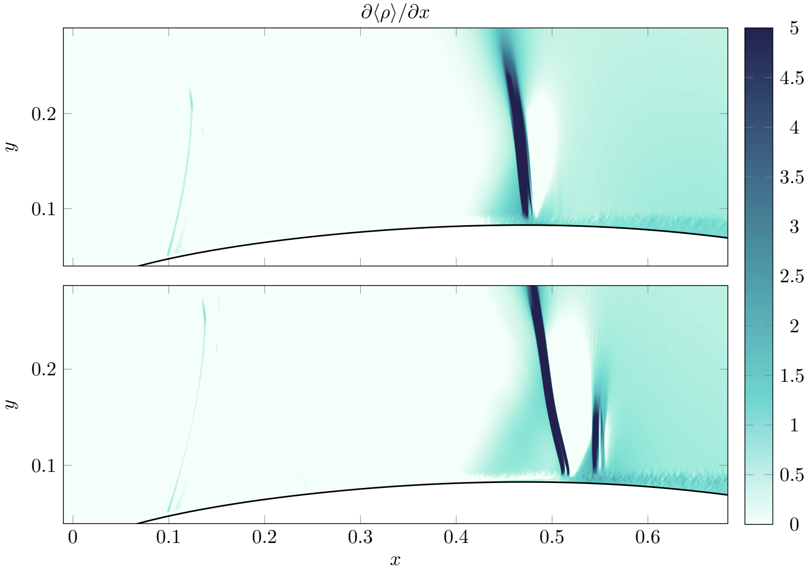

Separation

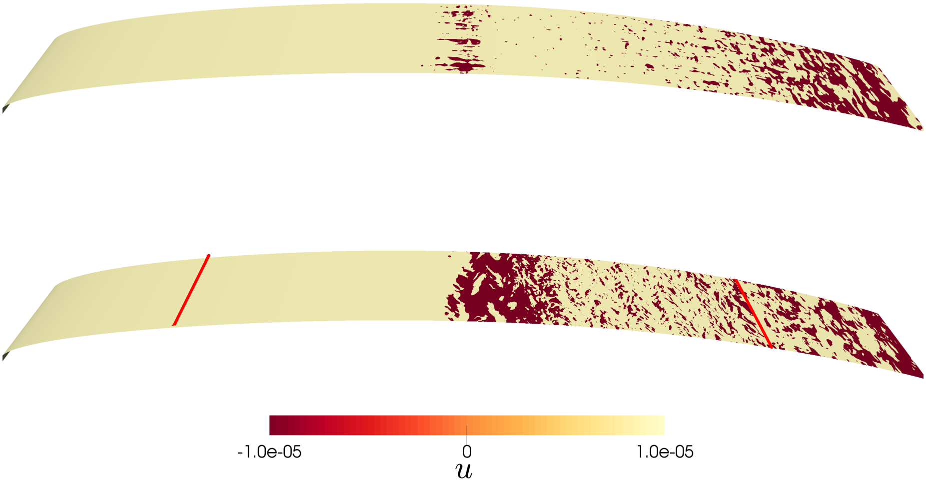

Bai et al. 2014

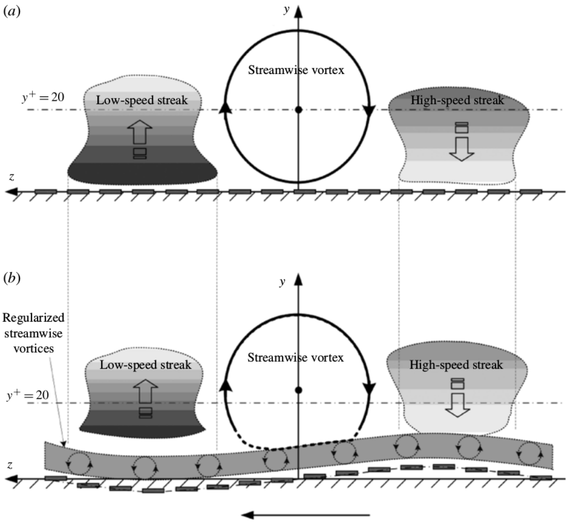

Channel with blowing

- $Re_\tau = 200$, $(L_x, L_y, L_z) = (31.4h, 3.2h, 2h)$, $(N_x, N_y, N_z) = (1050, 384, 200)$

Periodic

- $(L_x, L_y, L_z) = (2\pi h, \pi h, 2h)$
- $(N_x, N_y, N_z) = (210, 384, 200)$
- $(\Delta x^+, \Delta y^+, \Delta z^+_{lower}, \Delta z^+_{centre}, \Delta z^+_{upper}) = (6, 1.6, 0.3, 4, 0.3)$

Non-Periodic

- $(L_x, L_y, L_z) = (8\pi h, \pi h, 2h)$
- $(N_x, N_y, N_z) = (840, 384, 200)$
- $(\Delta x^+, \Delta y^+, \Delta z^+_{lower}, \Delta z^+_{centre}, \Delta z^+_{upper}) = (6, 1.6, 0.3, 4, 0.3)$

Non-uniform actuator

48 slits, $l_j^+ = 132$, $d_y^+ = 3.33$

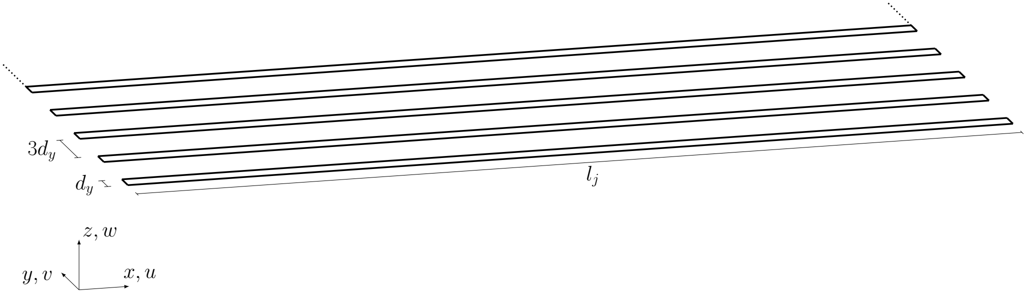

Simulations

Simulation	S_j/S_{tot}	f^+	W_w^+
U-S	1	–	0.355
NU-S	0.25	–	1.42
U-NS	1	0.14	1.775
NU-NS	0.25	0.14	7.1
StW	0.25	–	1.42

Table: Details of the blowing strategy employed. Here S_j/S_{tot} represents the fraction of the spanwise width covered by jets (unitary for uniform blowing); f^+ is the forcing frequency of the unsteady cases, W_w^+ is the blowing wall-normal velocity. The case StW investigates the blowing actuator over a spanwise-controlled wall by a standing wave with parameters $(A^+, \kappa_x^+) = (12, 0.01)$.

Blowing

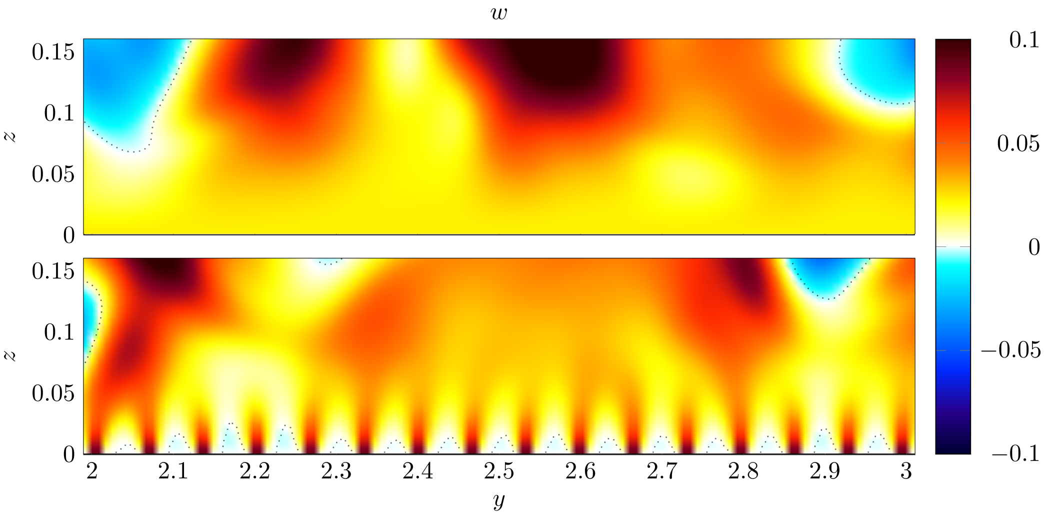
w
0.15
0.1
0.05
0
z
0.15
0.1
0.05
0
z
2
2.1
2.2
2.3
2.4
2.5
2.6
2.7
2.8
2.9
3
y
0.1
0.05
0
−0.05
−0.1

Blowing

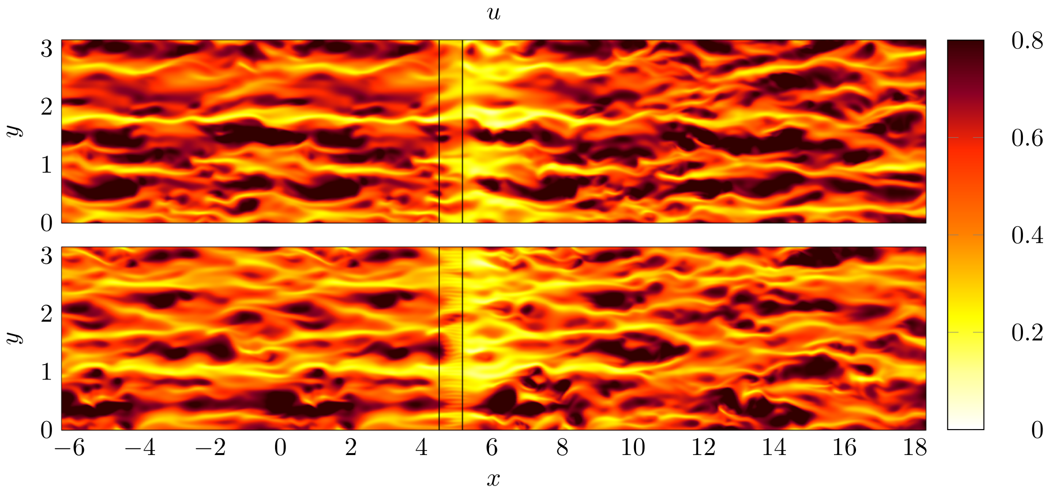

Blowing

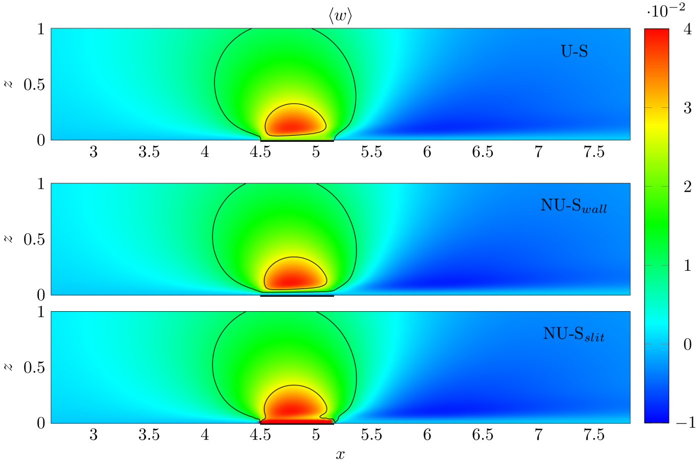

Colour plot of the mean wall-normal velocity w, for case U-S (top) and NU-S (bottom). The latter is shown over two planes: above the wall (second panel) and above the slit (third panel). Contour lines are drawn for $w = (0.01, 0.028)$.

Blowing

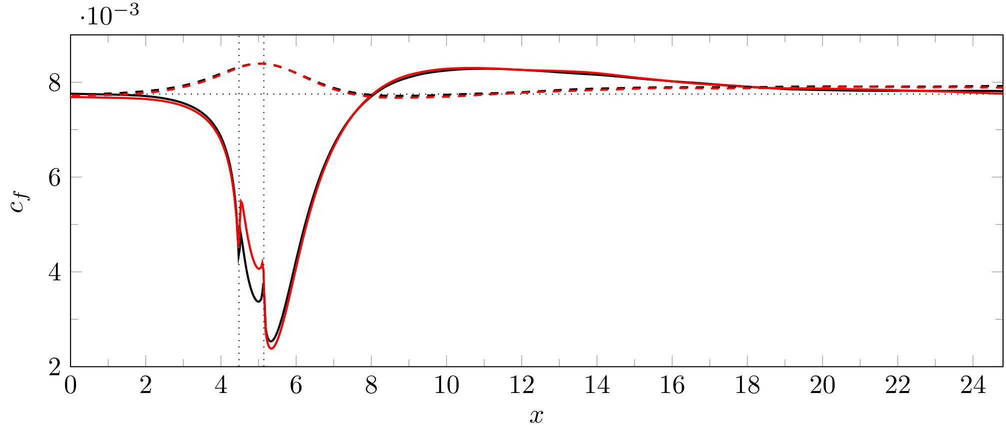

Skin-friction distribution $c_f(x)$: cases U-S (black) and NU-S (red) over the lower (solid lines) and upper (dashed lines) walls.

Blowing

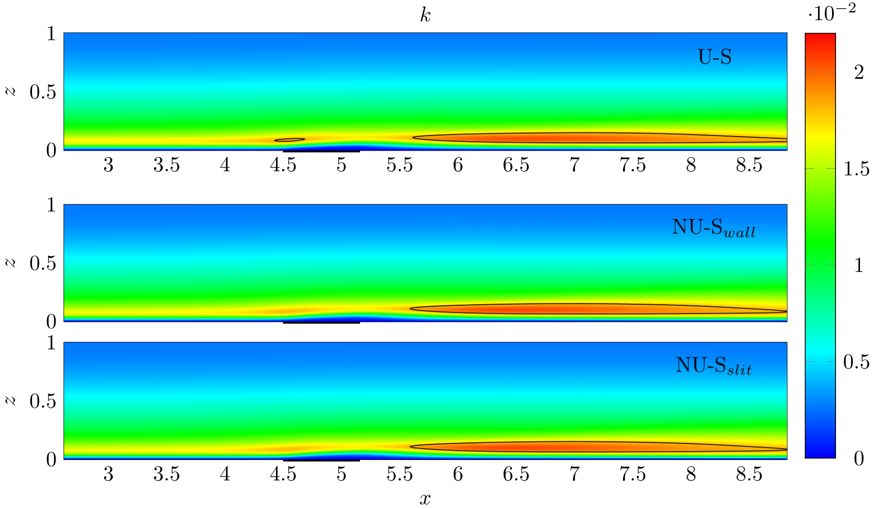

Colour plot of the turbulent kinetic energy, in outer units. Contour lines are drawn for k = 0.018.

Unsteady Blowing

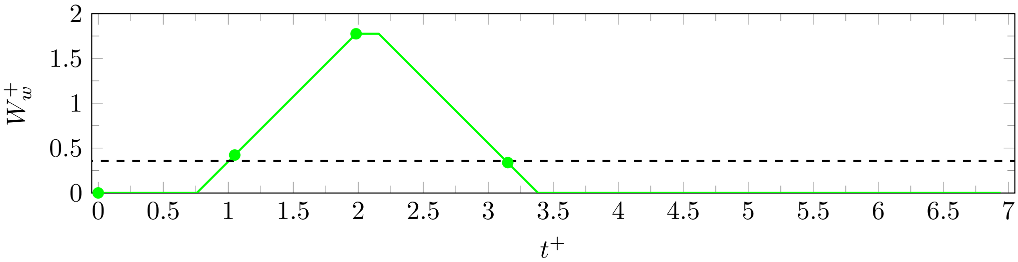

Temporal evolution of one period of the unsteady actuator U-NS (green). Four points underline the instants investigated in the following. The black dashed line denotes the steady forcing of case U-S.

Unsteady Blowing

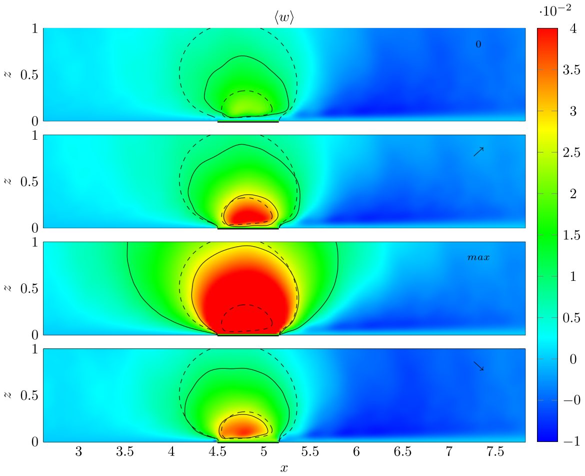

Colour plot of the mean wall-normal velocity w for case U-NS in four moments of the period: zero W_w, acceleration, maximum W_w and deceleration respectively. Contour lines are drawn for $w = (0.01, 0.028)$ for case U-NS (solid lines) and compared to the steady case U-S (dashed lines).

Unsteady Blowing

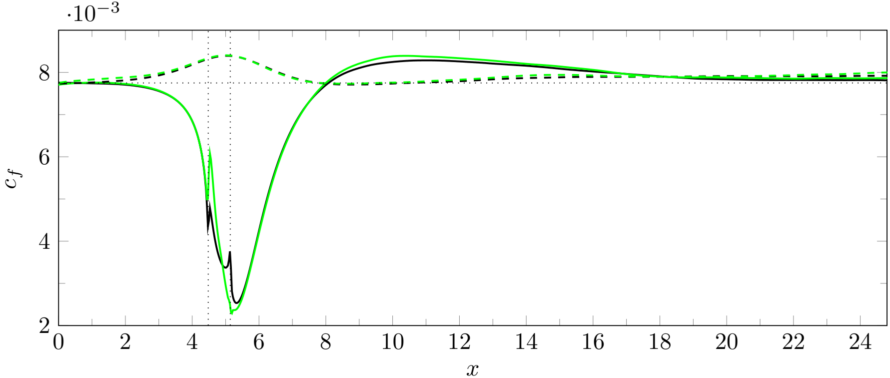

Skin-friction distribution $c_f(x)$: cases U-S (black) and U-NS (green) over the lower (solid lines) and upper (dashed lines) walls.

Unsteady Blowing

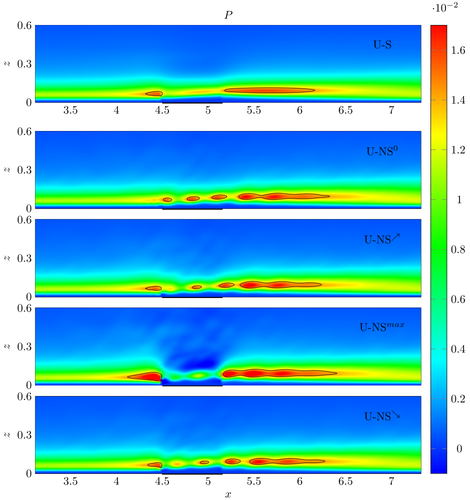

Colour plot of the production P of turbulent kinetic energy, for case U-S (top) and U-NS (bottom). The latter is shown in four instants of the forcing period. Contour lines are drawn for $P = (0.014)$.

Power Budget

	U-S	NU-S	U-NS	NU-NS
$P_{sav}\%$	3.29	3.23	2.8	1.72
$P_{req}\%$	0.0037	0.06	0.04	0.67
$P_{net}\%$	3.29	3.17	2.76	1.05

Table: Power budget for the four cases. P_{sav} is the power saved thanks to the reduction of friction drag. P_{req} is the power required for actuation, and $P_{net} = P_{sav} - P_{req}$ represents the net balance. Figures are for the lower wall only and are expressed as a percentage of P_{tot}, which is the power required to overcome the drag produced by the lower wall.

Blowing + Spanwise Forcing

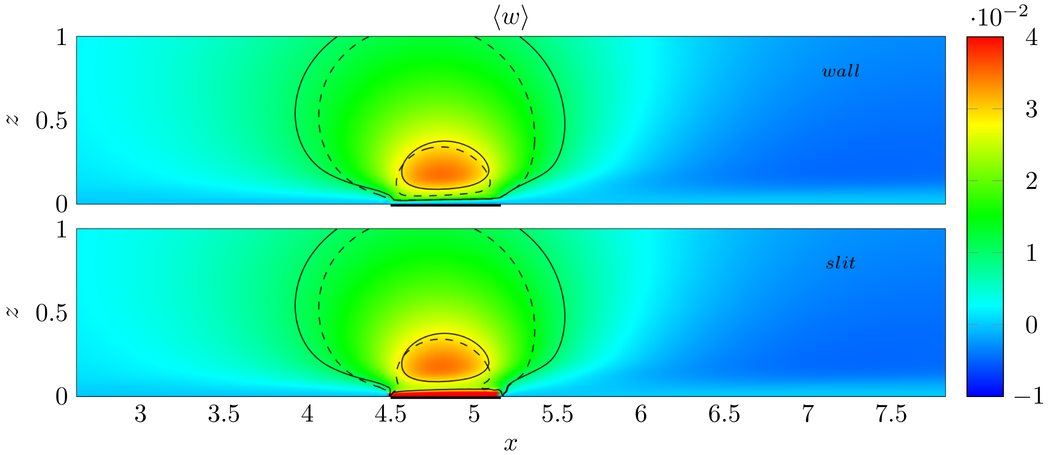

Colour plot of the mean wall-normal velocity w, for case StW over two planes: above the wall (first panel) and above the slit (second panel). Contour lines are drawn for $w = (0.01, 0.028)$ for case StW (solid lines) and compared to the steady case NU-S (dashed lines).

Blowing + Spanwise Forcing

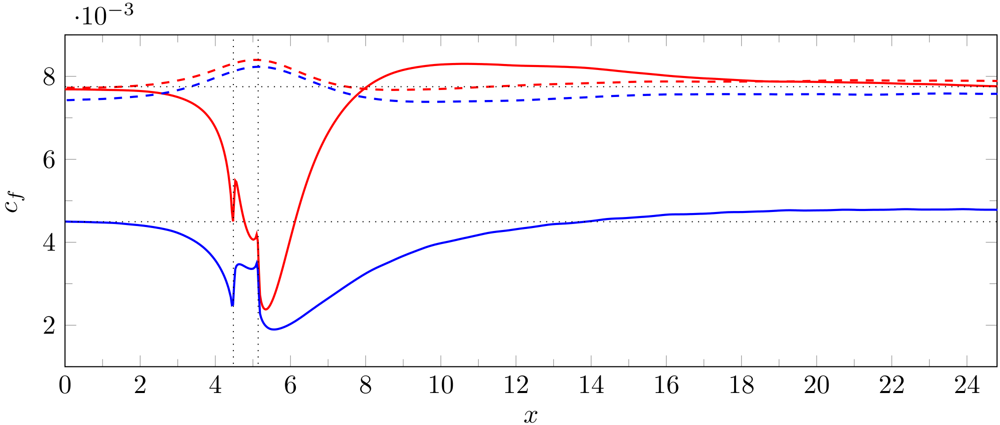

Skin-friction distribution $c_f(x)$: cases NU-S (red) and StW (blue) over the lower (solid lines) and upper (dashed lines) walls.

Blowing + Spanwise Forcing

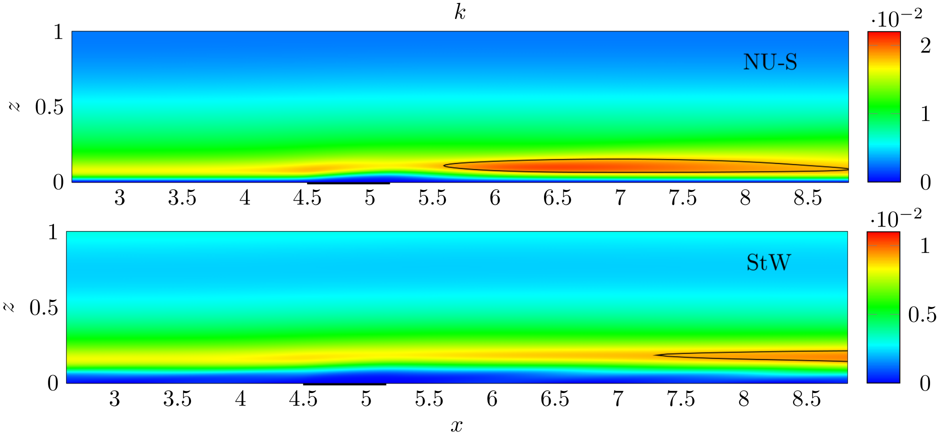

Colour plot of the turbulent kinetic energy, in outer units, for cases NU-S (top) and StW (bottom). Note the different colour-map scale. Contour lines are drawn at $k = 0.018$ for case NU-S and at $k = 0.009$ for case StW.

Blowing + Spanwise Forcing

$$\delta k = \frac{k}{max(k^p)} - 1,$$

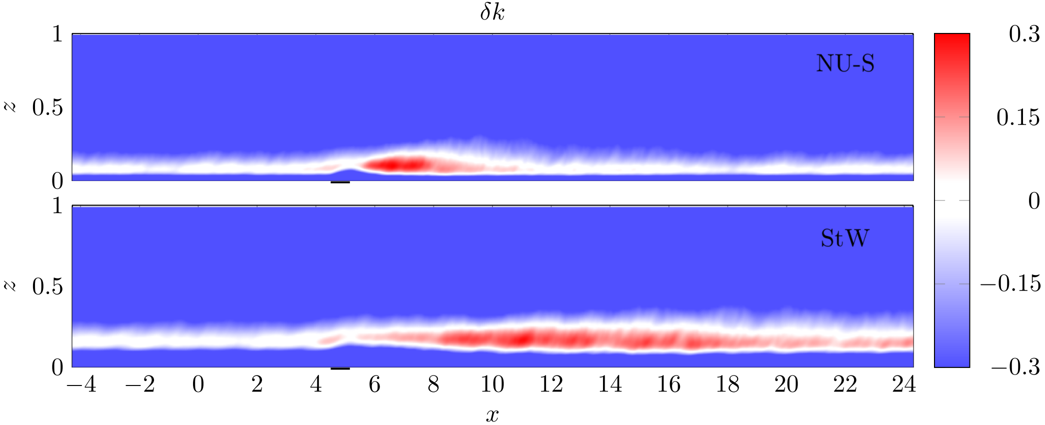

Colour plot of δk for case NU-S (top) and case StW (bottom).

Friction Prediction

When the topography modulation is shallow enough

- the response of the flow field is linear
- dimensionless shear stress perturbation $\delta\tau \ll 1$
- the problem can be addressed in $\widehat{\textit{Fourier}}$ space
- the Fourier-transformed $\widehat{\delta\tau}$ is proportional to $\widehat{h}$ via:

$$T(k^+) = \frac{\widehat{\delta\tau_{dim}/\tau_{dim}}}{\widehat{dh_{dim}/dx_{dim}}} = \frac{\widehat{\delta\tau}}{-ik\widehat{h}}$$

Friction Prediction

Luchini & Charru *JFM*17-19

$$\mathcal{T}^+(k^+) = \frac{\widehat{\delta\tau^+}}{\widehat{dh_w^+/dx^+}} = \frac{\widehat{\delta\tau^+}}{-ik^+\widehat{h_w^+}},$$

$$\mathcal{T}(k^+)^+ = \left[\frac{c_1}{c_2}(-ik^+)^{2/3} - i\frac{c_0}{c_2}(U_{\text{ext}}^+)^{-2}(-ik^+)^{-2/3}(k)\right]^{-1},$$

$$U_{\text{mean}}^+(z^+) = \frac{\log(z^+ + 3.109)}{0.392} + 4.48 - \frac{7.3736 + (0.4930 - 0.02450z^+)z^+}{1 + (0.05736 + 0.01101z^+)z^+}e^{-0.03385z^+}.$$

$$-ik^+\mathcal{T}^+(k^+) - 2k^+ = \frac{k^+ - 0.002087 - 0.000928i}{0.05220 + 0.03837i + (1.6592 + 1.2380i)k^+ + (-0.7009 + 1.2051i)(k^+)^2}$$

Friction Prediction - Laminar

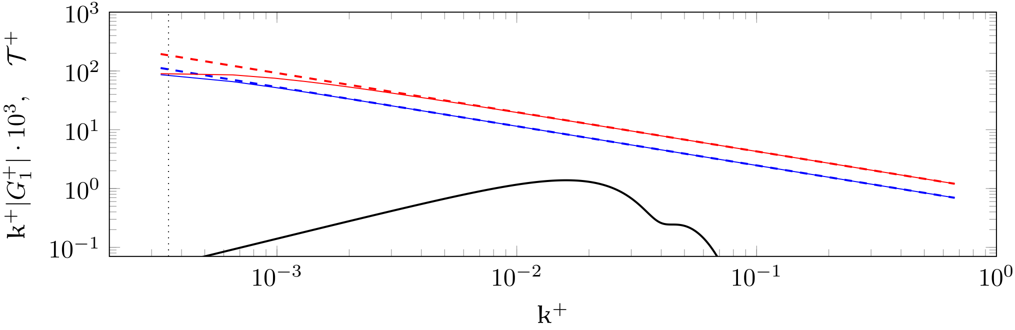

Module of the transformed wall-slope $k^+|\widehat{G_\mathbf{1}^+}|$ (black) and comparison between the asymptotic response function (solid lines) and classical theory benjamin-1959 (dashed lines): real (blue) and imaginary (red) components.

Friction Prediction - Laminar

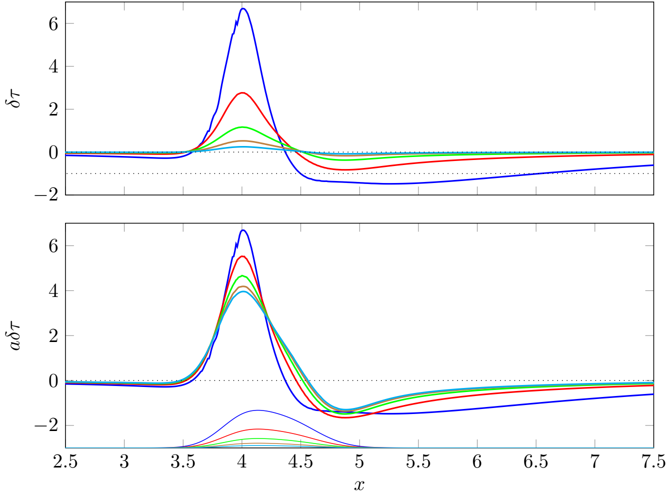

Wall-shear stress perturbation $\delta\tau$ for the five bumps $\frac{G_1}{a}$: $a = 1$ (blue), $a = 2$ (red), $a = 4$ (green), $a = 8$ (brown), $a = 16$ (cyan). Top: $\delta\tau$; bottom: $a\delta\tau$. The thin profiles at the bottom of the plot draw the five bump geometries.

Friction Prediction - Laminar

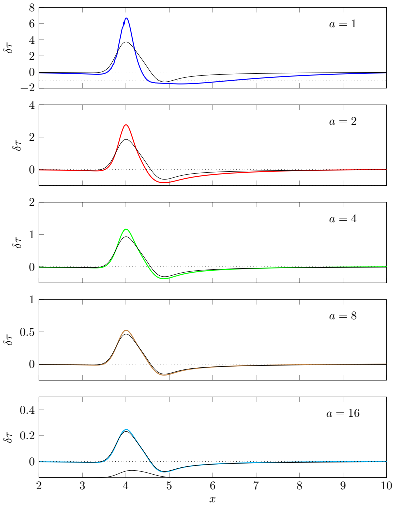

Wall-shear stress perturbation $\delta\tau$: computed (thick colour line) and predicted (thin black lines) for the five geometries. Note the vertical scale that is multiplied by $1/a$.

Friction Prediction - Laminar

a	$\Delta_M\%$	$\Delta_m\%$
1	45.5	$16(\Delta x_m = 0.37h)$
2	32.6	25.3
4	20.2	17.0
8	11	9.3
16	5.9	4.7

Table: Relative error for maximum (Δ_M) and minimum (Δ_m) of $\delta\tau$.

Friction Prediction - Turbulent

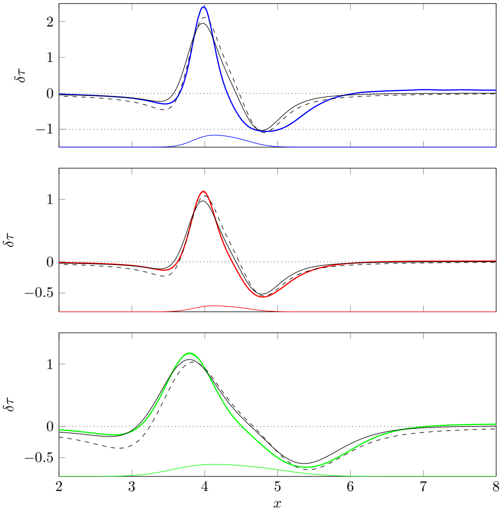

Wall-shear stress perturbation $\delta\tau$: computed (thick colour lines) and predicted via asymptotic (thin solid lines, black) and empirical (thin dashed lines, black) transfer functions. Top: $G_{\mathbf{1}}$; centre: $G_{\mathbf{1}h}$; bottom: $G_{\mathbf{1}L}$.

Friction Prediction - Turbulent

	$\Delta_{lm}\%$	$\Delta_M\%$	$\Delta_m\%$
G_1	23.5 (54.5)	19.0 (12.2)	2.5 (2.7)
G_{1h}	14.8 (72.2)	13.6 (6.3)	8.1 (3.2)
G_{1L}	19.4 (158)	8.7 (12.2)	9.1 (5.6)

Table: Relative error of the analytical and empirical prediction, for the local minimum (Δ_{lm}), the maximum (Δ_M) and minimum (Δ_m) of $\delta\tau$. Error via empirical transfer function is reported in parentheses.

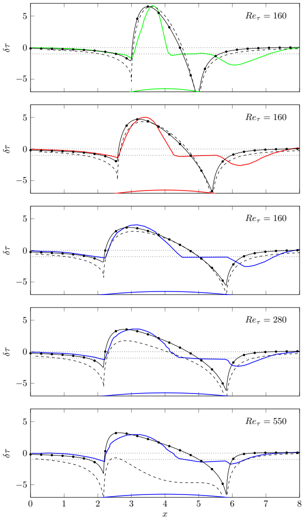
$Re_\tau = 160$
$Re_\tau = 160$
$Re_\tau = 160$
$Re_\tau = 280$
$Re_\tau = 550$
$\delta\tau$
x

Boundary layer

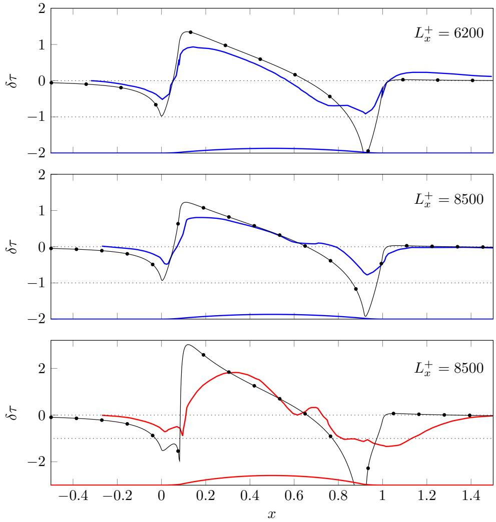

CHAPTER 6

LINEAR RESPONSE OF TURBULENT FLOWS OVER GENERIC BUMPS

Just because *we* don't understand something
doesn't mean that it's nonsense.

LEMONY SNICKET